Journal of Iberian Geology
https://doi.org/10.1007/s41513-024-00241-1

RESEARCH PAPER

The late Early Pleistocene site of Fuente Nueva-3 (Guadix-Baza Depression, SE Spain): a hyena latrine developed on a quicksand trap for megaherbivores?

Paul Palmqvist[1] · **Isidoro Campaña**[1] · **Alejandro Granados**[1] · **Bienvenido Martínez-Navarro**[2,3,4] · **Alejandro Pérez-Ramos**[1] · **Guillermo Rodríguez-Gómez**[5,6] · **Antonio Guerra-Merchán**[1] · **Sergio Ros-Montoya**[1] · **María Dolores Rodríguez-Ruiz**[7] · **José Manuel García-Aguilar**[1] · **Víctor Hernández**[8] · **M. Patrocinio Espigares**[1]

Received: 12 March 2024 / Accepted: 1 May 2024

Abstract

The late Early Pleistocene archaeological site of Fuente Nueva-3 (FN3), which lies in the Guadix-Baza Depression (SE Spain) and is dated to ~ 1.4 Ma, contributes some of the oldest evidence of hominin presence in Western Europe, including a huge tool assemblage of Oldowan tradition, manuports (i.e., unmodified stones used as percussion tools) and abundant fossils of large mammals, some of which preserve anthropogenic marks related to defleshing, butchering and marrow processing. In addition, there are bones with tooth marks produced by scavenging carnivores. The fertile layers of the FN3 section have been grouped in a lower archaeological level (LAL) and an upper archaeological level (UAL). Both levels preserve abundant skeletal remains and lithic tools. However, the LAL shows a high density of manuports, which suggests that hominin activity was more intense at this level, while the UAL preserves many remains of megaherbivores, particularly proboscideans (*Mammuthus meridionalis*), and almost all coprolites unearthed from the site, which points to a greater involvement of the giant hyenas (*Pachycrocuta brevirostris*). In this paper, we (i) test for statistical differences in the composition of the faunal assemblages preserved in the UAL and LAL; and (ii) analyze particle size in the fertile layers of both archaeological levels. Our results show that megaherbivores are comparatively overrepresented in the UAL, specially by young elephants, while other medium-to-large and large-sized ungulates, particularly equids, are more abundant in the LAL, showing a predominance of adult individuals. Concerning the sedimentology, layers 2–3 of the LAL show a predominance of silts and clays, with sands representing a minor fraction. In contrast, layer 5 of the UAL is composed of two-thirds of fine and very fine sands, with the remaining third consisting of silts and clays. These data and the paleoenvironmental reconstruction of layer 5 suggest that it may be interpreted as a paleo-quicksand in which megaherbivores were trapped due to the elevated weight per unit area supported by their feet, and their half-sunken carcasses attracted the scavengers, particularly the hyenas, which fed on these carcasses and defecated in their surroundings.

Keywords Orce · Early Pleistocene · Taphonomy · Paleoecology · Proboscideans · Coprolites

El yacimiento del Pleistoceno inferior de Fuente Nueva-3 (depresión de Guadix-Baza, sureste deEspaña): ¿Una letrina de hienas desarrollada en una trampa de arenas movedizas para la megafauna?

Resumen

El yacimiento arqueológico de Fuente Nueva-3 (FN3), de finales del Pleistoceno temprano, se sitúa en la Depresión de Guadix-Baza (SE de España) y ha sido datado en ~1,4 Ma. Aporta algunas de las evidencias más antiguas de la presencia de homininos en Europa occidental, incluyendo un amplio conjunto de herramientas de tradición olduvayense, manuports

---

Extended author information available on the last page of the article

(es decir, piedras no modificadas utilizadas como herramientas de percusión) y abundantes fósiles de grandes mamíferos, algunos de los cuales conservan marcas antropogénicas relacionadas con el desollamiento, la carnicería y el procesamiento del tuétano. Además, hay huesos con marcas de dientes producidas por carnívoros carroñeros. Las capas fértiles de la sección de FN3 se agrupan en un nivel arqueológico inferior (LAL) y un nivel arqueológico superior (UAL). Ambos niveles conservan abundantes restos óseos y herramientas líticas. Sin embargo, el LAL presenta una alta densidad de manuports, lo que sugiere que la actividad de los homininos fue más intensa en este nivel, mientras que el UAL conserva muchos restos de megaherbívoros, en particular proboscídeos (*Mammuthus meridionalis*), y casi todos los coprolitos exhumados del yacimiento, lo que apunta a una mayor participación de las hienas gigantes (*Pachycrocuta brevirostris*). En este trabajo (i) comprobamos si existen diferencias estadísticas en la composición de los conjuntos faunísticosconservados en el UAL y el LAL; y (ii) analizamos el tamaño de las partículas en las capas fértiles de ambos niveles arqueológicos. Nuestros resultados muestran que los megaherbívoros están comparativamente sobrerrepresentados en el UAL, especialmente por elefantes jóvenes, mientras que otros ungulados de tamaño medio-grande y grande, particularmente los équidos, son más abundantes en el LAL, mostrando un predominio de individuos adultos. En cuanto a la sedimentología, las capas 2-3 del LAL muestran un predominio de limos y arcillas, representando las arenas una fracción reducida. Por el contrario, la capa 5 de la UAL está compuesta en dos tercios por arenas finas y muy finas, y el tercio restante por limos y arcillas. Estos datos y la reconstrucción paleoambiental de la capa 5 sugieren que se puede interpretar como una paleoarena movediza en la que los megaherbívoros quedaban atrapados debido al elevado peso por unidad de superficie que soportaban sus extremidades, atrayendo sus cadáveres a medio hundir a los carroñeros, en particular a las hienas, que se alimentaron de estos cadáveres y defecaron en sus alrededores.

Palabras clave Orce · Pleistoceno inferior · Tafonomía · Paleoecología · Proboscidios · Coprolitos

1 Introduction and background

The late Early Pleistocene archaeo-paleontological site of Fuente Nueva-3 (FN3) lies in the north-eastern sector of the Guadix-Baza Depression (SE Spain, Fig. 1A–B), which is the largest intramontane basin of the Betic Cordillera (García-Aguilar and Palmqvist 2011; García-Tortosa et al. 2011; Palmqvist et al. 2022a). This inland basin extends over an area of ~ 4000 km^2 and is surrounded by the highest reliefs of the Alpine-Betic orogeny, which rise up to an altitude of ~ 3482 m above mean sea level (AMSL). During the Miocene, the sedimentary depression was connected to the Mediterranean Sea by the Almanzora Corridor and to the Atlantic Ocean by the Guadalquivir Basin. Both corridors were closed between the end of the Tortonian and the Lower Messinian, which led to a change from exorheic conditions to continental sedimentation in an endorheic basin (Soria et al. 1999; Hüsing et al. 2010). Isostatic uplifting, with an average uplift rate of ~ 200 m/Ma as estimated from Late Neogene coastal marine conglomerates and coral reefs (Braga et al. 2003), resulted in an elevation of the uppermost sedimentary level of the basin (i.e., the glacis geomorphological surface) to ~ 1000 m AMSL.

The Guadix-Baza Depression developed a network of endorheic drainage during most of the Pliocene and Pleistocene, being subject to intense tectonic subsidence in relation to the surrounding mountain ranges. This led to the accumulation of a ~ 550 m thick sedimentary record composed of lacustrine, alluvial and fluvial deposits (limestones, gypsum, marls, shales, sands, and conglomerates) Tectonically induced hydrothermal activity in the basin provided a mild and productive environment for the terrestrial fauna (García-Aguilar et al. 2014, 2015; Palmqvist et al. 2022a). This favored the development of rich and diverse paleocommunities of mammals through the Plio-Pleistocene, whose fossil remains were abundantly preserved in many paleontological and archaeological localities (Maldonado-Garrido et al. 2017; Martínez-Navarro et al. 2018; Palmqvist et al. 2022a). The Orce area (Fig. 1B–C), a satellite basin in the north-eastern sector of the depression with an extent of ~ 170 km^2, preserves a unique fossil record of the late Early Pleistocene (Late Villafranchian) fauna, including two archaeological sites dated to ~ 1.4 Ma that mark the earliest presence of hominins in Western Europe, Barranco León-D (BLD) and FN3 (Martínez-Navarro et al. 1997, 2014; Espigares et al. 2013, 2019, 2023; Toro-Moyano et al. 2013; Palmqvist et al. 2016, 2022a, 2023a).

The archaeological sites of BLD and FN3 preserve huge lithic assemblages of Oldowan (i.e., Mode 1) tradition (Barsky et al. 2015, 2016, 2022; Martínez-Navarro et al. 1997; Turq et al. 1996; Toro-Moyano et al. 2011, 2013; Titton et al. 2018, 2021) and abundant skeletal remains of vertebrates, particularly large mammals. Some of these fossils show anthropogenic marks related to defleshing, butchering and marrow processing (Espigares et al. 2013, 2019, 2023; Palmqvist et al. 2023a, 2023b; Yravedra et al. 2021, 2022). Moreover, a deciduous tooth of *Homo* sp. has been unearthed from BLD, which is by the moment the earliest hominin fossil from Western Europe (Toro-Moyano et al. 2013).

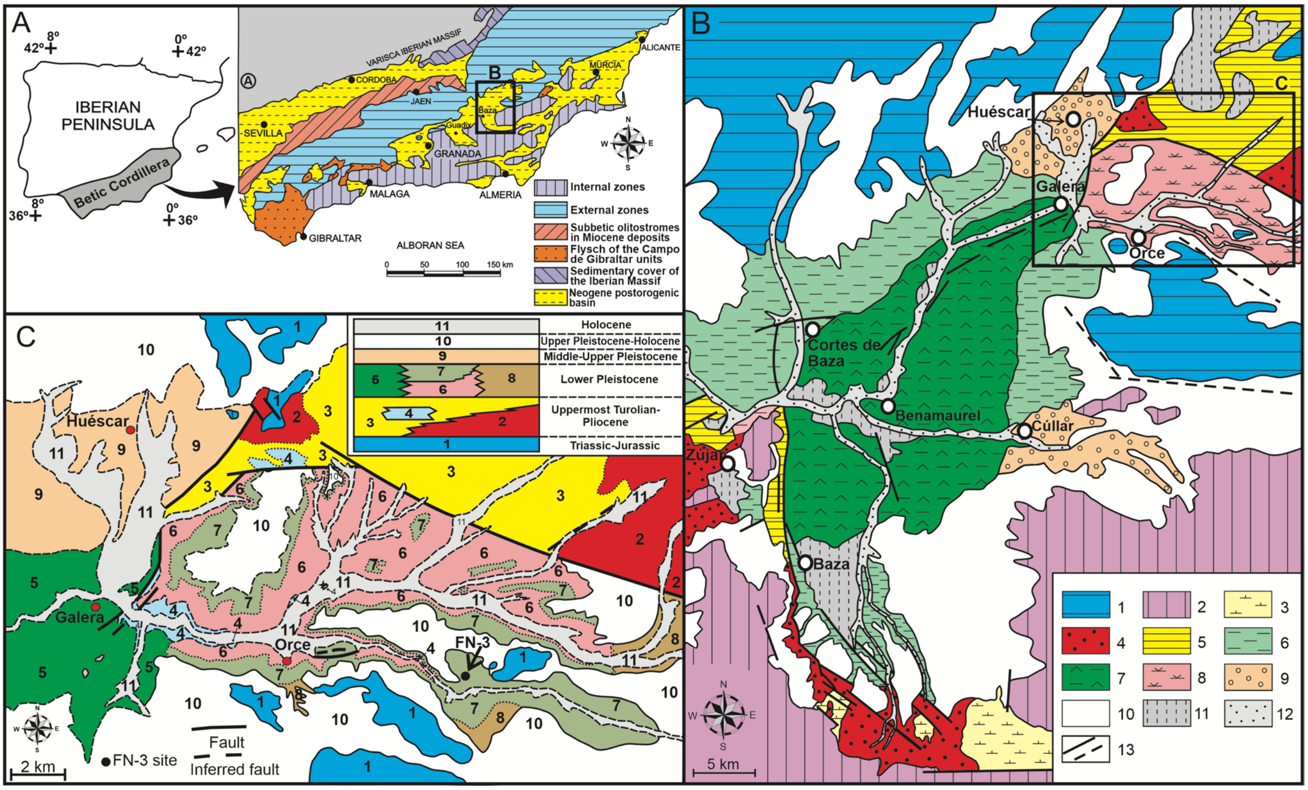

Fig. 1 **A** Geological context of the Baza Basin (SE Spain) within the Betic Cordillera (area marked by the rectangle). **B** Geologic map of the Baza Basin. 1- Substrate of the External Zones; 2- Substrate of the Internal Zones; 3- Tortonian, marine facies; 4- Plio-Pleistocene, alluvial facies; 5- Ruscinian-Lower Villafranchian, mainly lacustrine facies; 6- Lower and Middle Villafranchian, distal fluvial facies (sandstones and lutites); 7- Lower and Middle Villafranchian, marly-evaporitic lacustrine facies; 8- Late Lower Pleistocene lacustrine and fluvio-lacustrine facies; 9- Late Lower and Middle Pleistocene alluvial and lacustrine facies; 10- Glacis surface; 11- Recent alluvial; 12- Recent fluvial terraces and deposits; 13- Tectonic fractures (in discontinuous trace, inferred faults). **C** Geographic and geologic context of the Orce-Venta Micena sector in the Baza Basin. 1- Dolomites and limestones of the Subbetic domain (External Zones); 2- Red alluvial conglomerates; 3- Yellow lacustrine marls; 4- Lacustrine limestones; 5- Lacustrine marls, sands and gypsum; 6- Red and grey fluvial and lacustrine sands and clays; 7- Lacustrine marls and limestones; 8- Alluvial conglomerates; 9- Alluvial-deltaic conglomerates and sands, and lacustrine marls; 10- Glacis surface; 11- Recent fluvial gravels

There are several age estimates for BLD and FN3. For example, a combination of biostratigraphy, magnetostratigraphy and the U-series/ESR dating method applied to optically bleached quartz grains and fossil mammalian teeth provided age estimates of 1.43 ± 0.38 Ma for BLD and 1.19 ± 0.21 for FN3 (Duval et al. 2012; Toro-Moyano et al. 2013). In addition, an age of 1.50 ± 0.31 Ma was derived for FN3 based on cosmogenic nuclides (Álvarez et al. 2015). Moreover, the absence of suids from the rich faunal assemblages of BLD and FN3 contributes significant biochronological information (Martínez-Navarro et al., 2015): Suids are not present in Europe during the 1.8–1.2 Ma interval until the arrival of a derived form of *Sus strozzi* during the Epivillafranchian (Cherin et al. 2018, 2020). This species is first recorded in association with hominin remains at unit TE9 of Sima del Elefante in the Atapuerca karstic complex, which is dated to 1.22 ± 0.16 Ma on the basis of cosmogenic nuclides (Carbonell et al. 2008), and later in other sites of Jaramillo age like Untermassfeld in Germany, Vallonnet in France, or Vallparadís in Spain (Cherin et al. 2018, 2020; Madurell-Malapeira et al. 2010, 2014; Moullé et al. 2006). This proposal, however, has recently been challenged by Iannucci (2024) based on a distal fragment of a left suid Mt IV from a fossil collection of the XIX century. The specimen, which is housed in the Natural History Museum, London (NHMUK PV OR 27621), comes from Peyrolles, a locality of uncertain age of the French Central Massif. Although a fossiliferous level of Peyrolles has been dated by the ^{40}Ar/^{39}Ar method to 1.47 Ma (Nomade et al. 2014), it has been suggested that the short faunal list from this site is biochronologically coeval with the Upper Valdarno (Valli et al. 2006), which points to an age close to 1.8 Ma. Therefore, according to the evidence discussed above, the most parsimonious age for the two Orce sites, BLD and FN3, would be ~ 1.4 Ma (see review in Palmqvist et al. 2016).

The lithic assemblages unearthed from BLD and FN3 represent the whole reduction sequence. They are composed of abundant small flakes, debris, cobbles (one-third with percussion marks), cores, spheroids, and debitage made of flint, limestones and calcarenites from the site surroundings. Flint was largely exploited for flake production while limestone, although also used for flake production, was mostly employed as percussion tools (Barsky et al. 2015, 2016, 2022; Martínez-Navarro et al. 1997; Oms et al., 2000; Palmqvist et al., 2005; Toro-Moyano et al. 2011, 2013; Titton et al. 2018, 2021; Tixier et al. 1995; Turq et al. 1996). A small proportion of bones (< 2%) show cut marks and percussion marks resulting from defleshing and bone fracturing for accessing their marrow contents, respectively (Espigares 2010; Espigares et al. 2013, 2019; Palmqvist et al. 2023a; Yravedra et al. 2021). Incisions predominate among cut marks, although scrapes, sawing marks and chop marks are also documented. These marks evidence patterns of skinning, disarticulation, defleshing, evisceration, and periosteum removal. They concentrate on the bones of large and very large ungulates, like horses (*Equus altidens* and *Equus suessenbornensis*), megacerine deer (*Praemegaceros* cf. *verticornis*), bison (*Bison* sp.), rhino (*Stephanorhinus hundsheimensis*), hippo (*Hippopotamus antiquus*), and elephant (*Mammuthus meridionalis*). Evidence of intentional bone breakage includes percussion marks, pits, notches, impact flakes, and negative flake scars generated by a direct contact of the bones with the hammerstone (Espigares et al., 2019; Yravedra et al., 2021).

The faunal assemblages of BLD and FN3 also preserve bones with carnivore modifications. These bones are recorded in low proportions, like those with anthropogenic marks, and include tooth marks similar in morphology, dimensions and anatomical position to those found at the late Early Pleistocene site of Venta Micena (VM) in Orce, in which tooth marks are more abundantly represented (Courtenay et al., 2023; Espigares, 2010; Espigares et al., 2019; Palmqvist et al., 2023b; Yravedra et al., 2021). The VM site, which is dated by biostratigraphy to 1.6–1.5 Ma (Martínez-Navarro, 1991; Palmqvist et al., 2022b), has been interpreted as a breeding den of the giant, short-faced hyena *Pachycrocuta brevirostris* (Arribas & Palmqvist, 1998; Espigares, 2010; Palmqvist & Arribas, 2001; Palmqvist et al. 1996, 2011, 2022b). For this reason, most tooth-marked bones of BLD and FN3 were probably also consumed by *P. brevirostris* (Espigares et al. 2013, 2019, 2023; Palmqvist et al., 2023a, 2023b). However, some activity of small carnivorans has also been identified in these sites (Espigares, 2010; Espigares et al., 2013, 2019), probably the medium-sized canid *Canis mosbachensis* (Courtenay et al., 2023; Palmqvist et al., 2023b). Moreover, a bone shaft from FN3 was apparently gnawed by a porcupine (Espigares et al., 2019).

The activity of *P. brevirostris* is particularly evident in the case of the upper archaeological level of FN3, in which hyena coprolites are abundantly preserved (Espigares, 2010; Espigares et al., 2019, 2023), as explained below. Apart from this large hyaenid, carnivores are well represented in BLD and FN3, including two mustelids (*Martellictis ardea* and *Meles meles*), three canids (*Vulpes alopecoides, C. mosbachensis,* and *Lycaon lycaonoides*), one ursid (*Ursus etruscus*), and three felids (*Lynx pardinus, Megantereon whitei* and *Homotherium latidens*) (Martínez-Navarro et al., 2010; Palmqvist et al., 2023a; Rodríguez-Gómez et al., 2016a, 2016b; Ros-Montoya et al., 2021). This rich carnivore guild resembles those found in other late Early Pleistocene archaeological and paleontological sites of Eurasia, such as Dmanisi in Georgia, dated to ~ 1.8 Ma (Medin et al., 2019; Bartolini-Lucenti et al., 2021, 2022), Pirro Nord in Italy, dated to 1.6–1.3 Ma (Petrucci et al., 2013), and Vallonnet in France, dated to ~ 1.1 Ma (Moullè et al., 2006), or at the early Acheulian site of ‘Ubeidiya in Israel, dated to 1.6–1.2 Ma (Martínez-Navarro et al., 2009).

The lithic assemblages of BLD and FN3, together with the inferences on the availability of animal resources and the intensity of competition among carnivores and hominins for these resources (Rodríguez-Gómez et al., 2016a, 2016b, 2022, 2024), provide interesting clues on the subsistence strategies of the first human populations that colonized Western Europe during late Early Pleistocene times (Espigares et al., 2013, 2019; Palmqvist et al., 2022a, 2023a; Rodríguez-Gómez et al., 2016a, 2017, 2022, 2024; Toro-Moyano et al., 2013).

1.1 The late Early Pleistocene site of FN3

The stratigraphy of FN3 consists of a ~ 5 m thick section formed by the alternation of sub-horizontal limestones with lutites and fine sands. This stratigraphic section was first described by Turq et al. (1996) and later by Oms et al. (2011), who described twelve layers (see Fig. 2A–C), numbered from bottom to top and grouped into three sedimentary cycles. Each cycle begins in a lower part constituted by greenish marly lutites and clays, as well as sands with iron oxides and carbonate nodules, and ends in an upper part characterized by a limestone/marly limestone stratum with evidence of microkarstification, together with intraclasts and diagenetic markers (Fig. 2D). These lutitic-carbonate sediments were deposited in a shallow lacustrine-to-swampy environment of variable depth, with occasional fluvial inputs (Turq et al., 1996; Oms et al., 2011; Espigares et al., 2023). Specifically, the clays and marly lutites were deposited under a semi-permanent water table while the sands correspond to lake shore deposits.

The first sedimentary cycle is only represented by its upper part (layer 1), a whitish limestone stratum with a

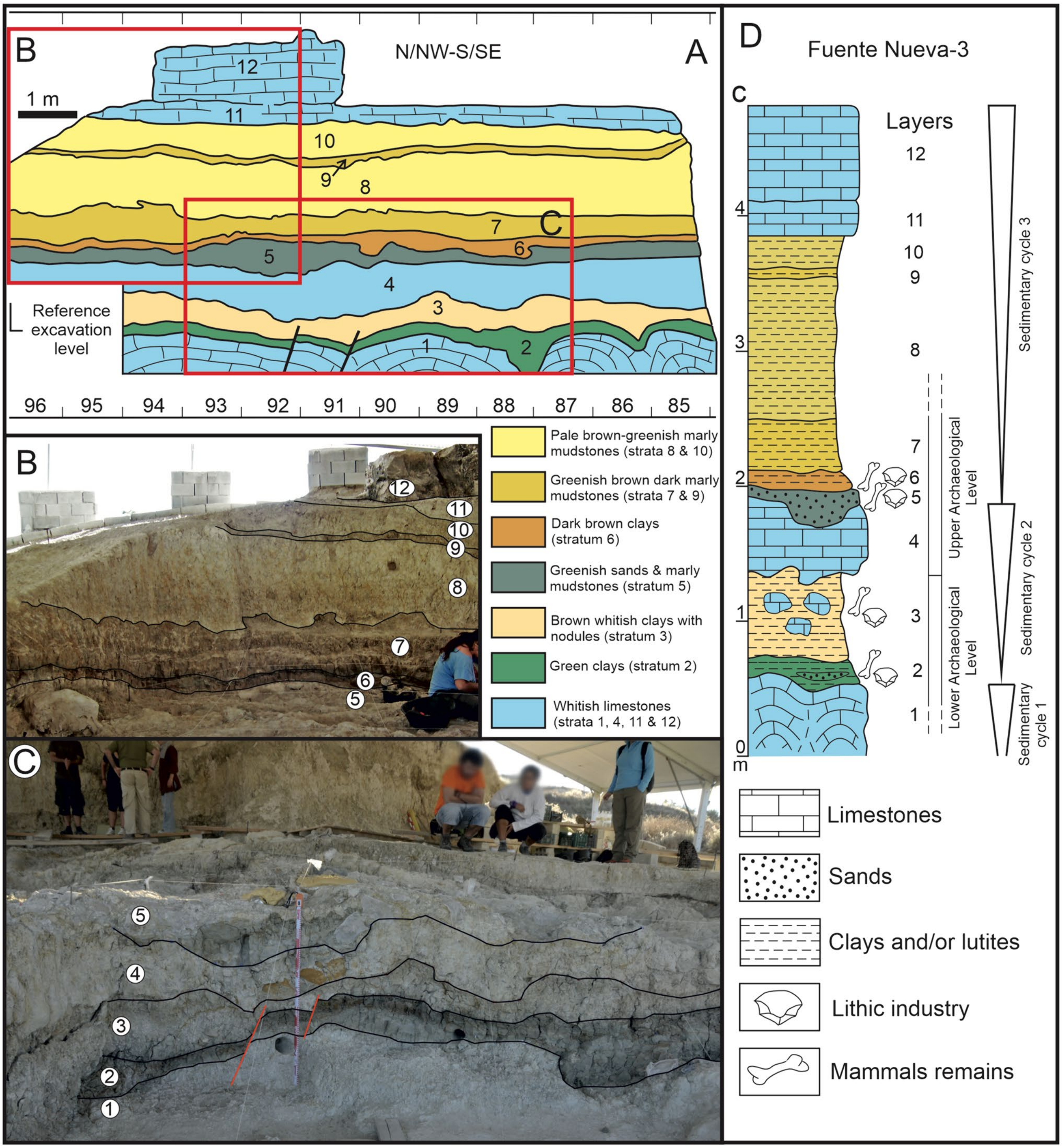

Fig. 2 **A** Stratigraphic scheme of the layers of the Fuente Nueva-3 (FN3) site (modified from Oms et al., 2011; Fig. 6; Espigares et al., 2023: Fig. 2). This stratigraphy shows a succession of layers constituted by whitish nodular limestones (layers 1, 4, 11, and 12) and irregular layers of yellowish marly lutites (layers 2–3 and 6–10), as well as dark greenish sands that appear in an intermediate position (layer 5). All these layers show evidence of subaerial pedogenesis and can be grouped into three sedimentary cycles (Espigares et al., 2023; Oms et al., 2011; Palmqvist et al., 2023a). **B** Image showing the morphology of the upper layers (4–7), which constitute the upper archaeological level (UAL). **C** Image showing the morphology of the lower layers (1–3), which represent the lower archaeological level (LAL). Red lines indicate faulting. **D** Stratigraphic series of the FN3 site

soft-sediment deformation structure that shows a rounded, pillow-shaped surface (Fig. 3). The second cycle (layers 2–4) and the third (layers 5–12) are both preserved complete. Layer 2 is an irregular bed of green clays that conforms to the surface of layer 1, showing a similar soft-sediment deformation structure. This layer is of variable thickness (10–20 cm) and includes small intercalations of sand. Layer 3 was deposited in concordance with layer 2 and consists of brown-whitish clays with carbonate nodules. Layers 1–3 show plastic deformation and small syn-sedimentary normal faults with a vertical extent of a few centimeters (Fig. 2C). In all probability, these structures were formed by earthquakes (Oms et al., 2011), which are frequently recorded in the Baza Basin (Alfaro et al., 1997, 2010; Gibert et al., 2005). Layer 4 is a whitish limestone that seems to have been less affected by deformation. The bottom of this layer conforms to the paleosurface, while its top is eroded by the deposition of the overlying sediments. The third sedimentary cycle consists of layers 5–12 (Fig. 2B). Layer 5 is of variable thickness (20–30 cm, although it can occasionally be thicker) and consists of greenish sands with lenticular shapes, which can be interpreted as the result of low-energy fluvial flows with sufficient energy to erode the unconsolidated limestones of layer 4. A high percentage (68.2%, 5466 out of 8014) of the fossil remains of large mammals unearthed from FN3 are from layer 5 (Espigares et al., 2023: Table 1). Layers 6–10 are composed of marly lutites and clays, which show differences in color and thickness. The boundary between layers 7 and 8 shows an important irregularity, which may be indicative of an erosional process resulting from subaerial emersion. Finally, layers 11–12 are horizontal whitish

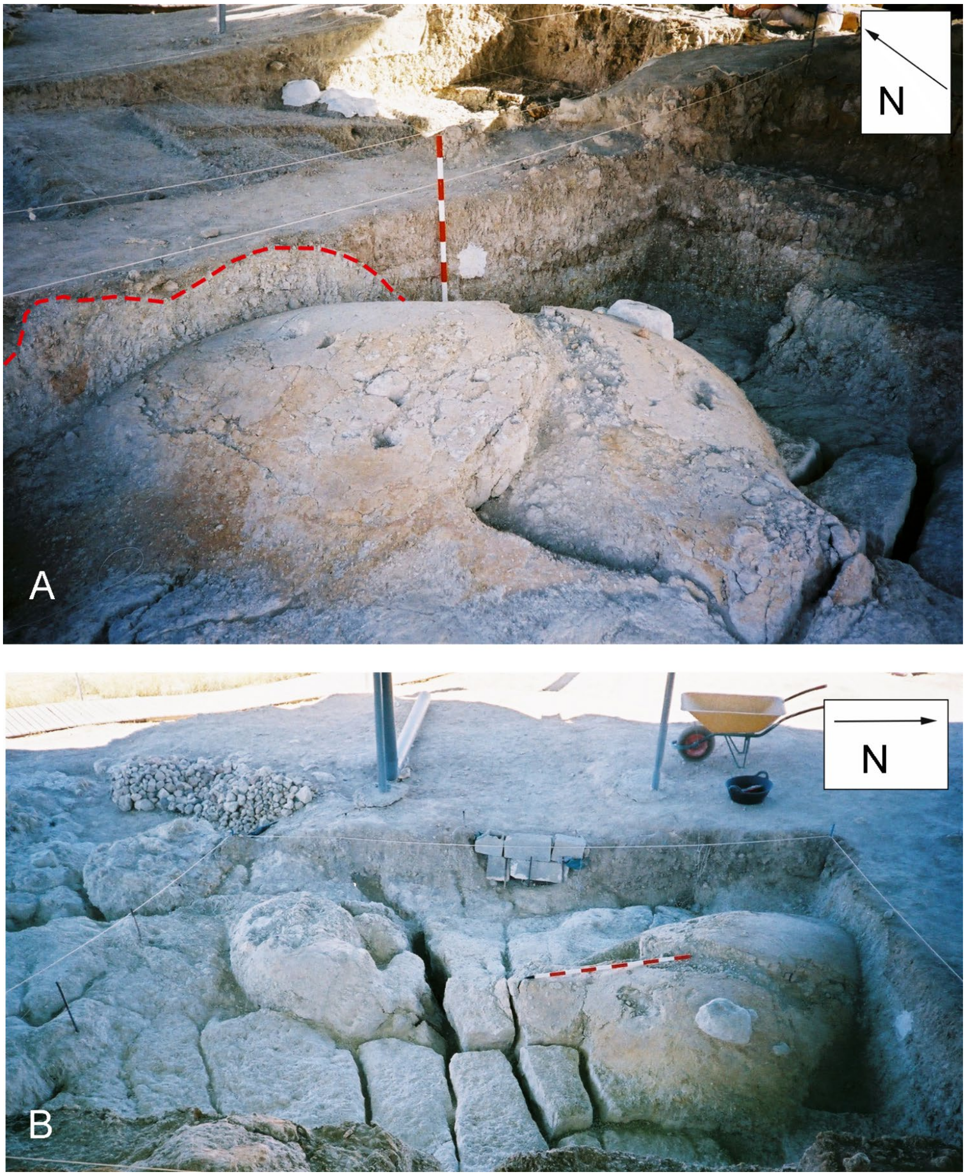

Fig. 3 Basal limestones (layer 1) of the Fuente Nueva-3 (FN3) site showing dome-shaped deformation structures, which were probably caused by an earthquake (photographs taken during the excavation season of the year 2003). **A** View of the dome structure with an approximately E-W orientation. The red dashed line to the northern wall shows that the overlying layers adapt to the morphology of the limestones. **B** Top view of the basal limestones showing two dome-shaped structures and abundant fractures. Similar dome-shaped structures figured by Gibert et al. (2005) were interpreted as paleoseismites

Table 1 Vertebrate assemblage unearthed from the Fuente Nueva-3 (FN3) site during the systematic excavations of the years 1999–2015 (data from Espigares et al., 2019: Tables S7–S8) and 2017–2020 (data from Yravedra et al., 2021: Table 1) distributed according to archaeological levels

FN3	Espigares et al. (2019)						Yravedra et al. (2021)			
	Lower archaeological level		Upper archaeological level		Indeterminate Level		Lower archaeol. level		Upper archaeol. level	
Taxa (estimated body mass)	NISP	MNI (j/a)	NISP	MNI (j/a)	NISP	MNI (j/a)	NISP	MNI	NISP	MNI
Homotherium latidens (200 kg)					1	1 (0/1)				
Lynx cf. *pardinus* (18 kg)			2	1 (0/1)						
Pachycrocruta brevirostris (110 kg)	3	1 (0/1)	7	2 (0/2)						
Lycaon lycaonoides (30 kg)	1	1 (0/1)	3	1 (0/1)	1	1 (0/1)				
Canis mosbachensis (12 kg)	5	1 (0/1)	10	1 (0/1)						
Vulpes alopecoides (5 kg)	2	1 (0/1)	7	2 (0/2)						
Ursus etruscus (300 kg)	3	1 (0/1)	25	2 (0/2)	4	1 (0/1)			3	1
Meles meles (15 kg)			3	1 (0/1)						
Martellictis ardea (7 kg)			2	2 (0/2)	1	1 (0/1)				
Carnivore indet							1	1	3	1
Total carnivores	14	5 (0/5)	59	12 (0/12)	7	4 (0/4)	1	1	6	2
Mammuthus meridionalis (6000 kg)	66	2 (2/0)	344	8 (6/2)	60		1	1	392	5
Stephanorhinus hundsheimensis (1000 kg)	13	1 (0/1)	108	5 (2/3)	30	1 (0/1)	1	1	19	3
Equus altidens (350 kg)	321	14 (5/9)	75	4 (1/3)	232	10 (0/10)			5	1
Equus suessenbornensis (565 kg)	17	2 (0/2)	4	2 (1/1)	13	2 (0/2)				
Equus sp.	37	3 (1/2)	170	7 (2/5)	4	1 (0/1)	3	2	27	2
Hippopotamus antiquus (3200 kg)	24	1 (0/1)	144	4 (2/2)	27	1 (0/1)			53	3
Bison sp. (450 kg)	27	3 (0/3)	51	6 (1/5)	64	1 (1/0)			8	2
Hemibos sp. cf. *H. gracilis* (300 kg)	1	1 (0/1)	1	1 (0/1)						
Hemitragus albus (75 kg)	14	4 (1/3)	19	3 (0/3)	10	2 (0/2)			6	1
Ammotragus europaeus (135 kg)					2	1 (0/1)				
Bovidae indet							4	2	20	3
Praemegaceros cf. *verticornis* (385 kg)	23	1 (0/1)	87	4 (1/3)	35	2 (0/2)	1	1	5	1
Metacervoceros rhenanus (95 kg)	46	4 (2/2)	17	3 (1/2)	26	2 (0/2)	1	1	2	1
Cervidae indet							1	1	36	3
Megaherbivores (> 1000 kg)	103	4 (2/2)	596	17 (10/7)	117	2 (0/2)	2	2	464	11
Other herbivores (< 1000 kg)	486	32 (9/23)	424	30 (7/23)	386	21 (1/20)	10	7	109	14
Large mammals (> 5 kg)	603	41 (11/30)	1079	59 (17/42)	510	27 (1/26)	13	10	579	27
Oryctolagus cf. *lacosti*	3		9						6	
Mammal indet	213		700		36		30		369	
Chelonia indet	18		36		3				35	
Aves indet	2		4		1				1	
Non-identified elements (mostly bone shafts)	1235		4086		301		165		3606	

Abundances of large mammals are reported as numbers of identifiable specimens (NISP) and estimates of minimum numbers of individuals [MNI, juveniles/adults (j/a)]

limestones that close the third sedimentary cycle and the stratigraphic section of FN3.

From an archaeological point of view, the fertile strata of FN3 have a thickness of ~ 1.5–2 m and comprise the first seven layers, which have been grouped in two main archaeological levels (Turq et al., 1996; Martínez-Navarro et al., 1997; Oms et al., 2011; Espigares et al. 2013, 2019, 2023; Reinoso et al., 2020; Palmqvist et al., 2023a): The lower archaeological level (LAL, layers 1–3) and the upper archaeological level (UAL, layers 4–7). Fossil bones, hyena coprolites, lithic tools, and manuports have been recovered from six different layers of FN3, although most of them come from layers 2–3 of the LAL and layer 5 of the UAL (Espigares et al., 2023: Table 1). Up to the 2015 excavation season, 1367 Mode 1 lithic artifacts knapped in situ were unearthed from FN3. In addition, there are 375 unmodified stones or manuports (i.e., non-flaked, allochthonous blocks and cobbles from the Jurassic carbonate rocks of the site surroundings). Nearly half of these limestone blocks display percussion marks (Barsky et al., 2015, 2016, 2022), which suggests they were probably intentionally brought to the FN3 site by the hominins, who used them as percussion tools for fracturing the bones of large mammals.

In a recent study, Espigares et al., (2023: Table 1) showed that fossil bones and lithic tools are abundantly preserved in both archaeological levels of FN3 (see Fig. 4): 2234 bones and 507 lithic tools come from the LAL, while 5780 bones and 482 tools are from the UAL. However, there are differences between both archaeological levels. For example, the density of manuports is higher in the LAL than in the UAL: 329 out of 375 manuports (87.7%) come from layers 2–3 of the LAL and only 46 (12.3%) from layer 5 of the UAL. This suggests that hominin activity concentrated in the LAL. In contrast, hyena coprolites are more abundantly represented in the UAL than in the LAL (Fig. 4): 98.2% (216 out of 220) coprolites preserved in FN3 come from layer 5 of the UAL and only three were recovered from layers 2–3 of the LAL (Espigares et al., 2023: Table 1). This suggests that hyaenid activity was particularly intense at the UAL.

According to Espigares et al. (2023), the lithological differences between the LAL and UAL could tentatively explain the differences in the composition of their bone assemblages of large mammals. Specifically, the fossiliferous layers of the UAL (layers 5–7; see Fig. 2) are composed of greenish fine sands and marly mudstones (layer 5), dark brown clays (layer 6), and greenish-brown dark marly mudstones (layer 7). In contrast, the fertile layers of the LAL (layers 2–3) are composed of green clays (layer 2) and brown whitish clays with nodules (layer 3). The composition of layer 5, which preserves most of the skeletal remains from the UAL, led Espigares et al. (2023) to propose that this layer could have behaved as quicksand that became unstable when it was forced to move by the pressure exerted by very large sized animals like megaherbivores, which remains are particularly abundant in this layer. For this reason, Espigares et al. (2023) interpreted layer 5 of the UAL, which preserves a high number of hyena coprolites, as a latrine of the giant hyena *P. brevirostris* developed in an open-air setting.

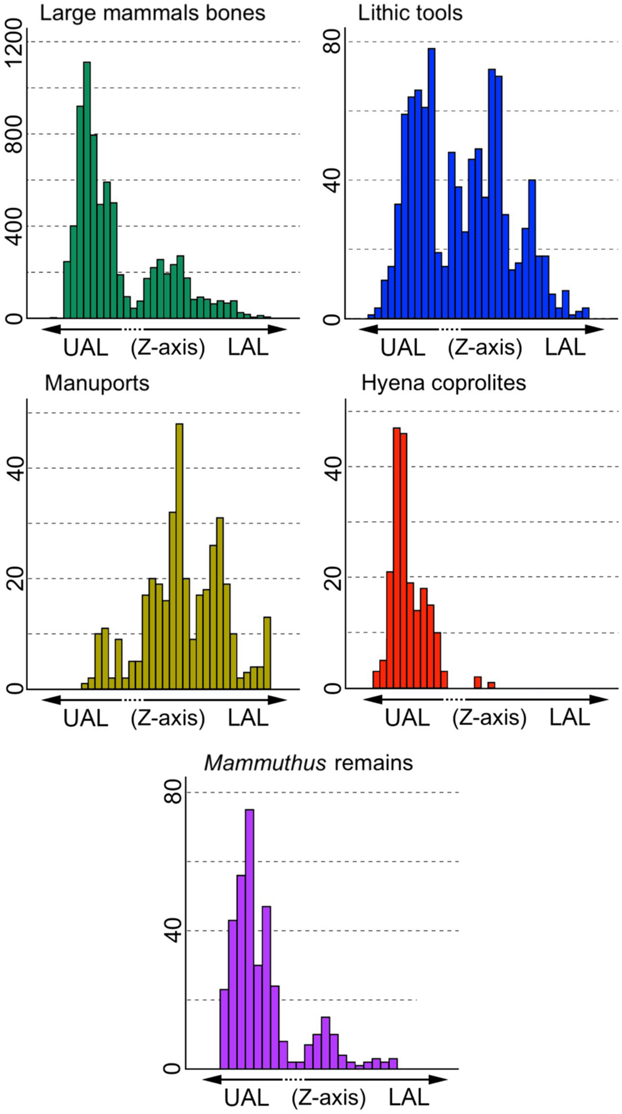

Fig. 4 Abundance (*Z*-axis) in the two archaeological levels of the late Early Pleistocene site of Fuente Nueva-3 (FN3) of fossil remains (mostly large mammals; see Table 1), lithic tools (flakes, debris, cobbles, and debitage), manuports (unmodified limestone blocks intentionally brought to the site by the hominins), hyena coprolites, and skeletal remains of elephant *Mammuthus meridionalis* (data from Espigares et al., 2023: Figure 12 and Table 1). The limit of the layers included in the upper archaeological level (UAL, layers 4–7) and lower archaeological level (LAL, layers 2–3) is not depicted in this figure, because these layers show irregular bedding surfaces (see Fig. 2)

1.2 Quicksand as a potential deadly trap for megafauna

Quicksand can potentially be a deadly trap for wildlife. Given its composition (fine sand, silt and salt water), quicksand is extremely sensitive to even small changes in stress, which can result in significant variations in its steady-state viscosity, thus causing the sediment to liquefy. For this reason, the higher the stress, the more fluid the quicksand becomes, so movement by a trapped body causes it to sink (Khaldoun et al., 2005, 2006). After an animal sinks into quicksand, the viscosity of the sediment increases due to the separation of the quicksand into two phases: a water-rich phase and a sand-rich phase (Khaldoun et al., 2005). This causes an animal trapped in quicksand to sink deeper when it moves trying to escape from the quicksand trap (Khaldoun et al., 2005). In such an environment, viscosity can reach such high levels that an animal may require a force up to three times its weight to free itself from the sediment (Kadau et al., 2009).

If artesian conditions exist, quicksand is formed by spring water issuing from an underlying permeable stratum fed by a head of water at higher elevation (Matthes, 1953). Surface quicksand is likely to occur in hilly country, especially in regions of calcareous rocks like the Baza Basin, which often contain solution openings, thus favoring the occurrence of springs (Patchick, 1966). In these environments, the sun bakes a thin crust on the sand (Matthes, 1953), which hides the risk of this substrate for animals moving in the vicinity.

The coefficient of friction and the penetration hardness of a quicksand depend on the water contents it incorporates (Fall et al., 2014; Liefferink et al., 2020). At low water contents the sand shows a pendular regime and can withstand relatively high loads before reaching the critical penetration hardness. Deformation of the granular material causes a reorientation of the grains, including the breaking and rebuilding of capillary liquid bonds. An increase in water content causes coalescence of the liquid bonds and a shift to a capillary regime, which further decreases the plastic response of the granular material. As a result, the coefficient of friction increases, resulting in an increased risk of entrapment for heavy animals with large limb sections. In addition, the high body mass of a trapped megaherbivore like an elephant makes it more difficult for it to counteract the negative suction of the quicksand to lift its pillar-like legs out of the sand (see Ren et al., 2010). In this scenario, an increase in salinity increases the cohesion and viscosity between the sand grains, which in turn increases the hardness of penetration into the quicksand (Fall et al., 2014). In a warm region like the Baza Basin, the evaporation of water from a sand with salt water results in the formation of salt crystals that fill the spaces between the sand grains. This process binds the sand grains together more tightly, creating a stiffer material that is more resistant to penetration stresses. The increase in strength is particularly noticeable in the pendular regime, where the amount of water (and thus dissolved salt) is relatively low but sufficient to form liquid bridges which, when evaporating, leave salt crystals that function as solid bridges in the surface crust. This is a double-edged trap because the surface crust is fragile. For this reason, if the fracture limit at the surface is exceeded (Nguyen et al., 2016), a death trap occurs when the limbs of a large sized animal move into the sand layer with an elevated water content, where the penetration hardness is lower and the friction is higher, thus trapping the animal. This would explain the difference of behavior between the LAL and UAL of FN3, and also why hyenas and hominins were able to roam the surface of quicksand without facing excessive risk of sinking into it, as explained below.

Experimental data on quicksand from salt-lake environments composed of fine sand, clay and salt water, similar in composition to those found in the sediments deposited in the oligosaline lacustrine systems recorded at the Orce sites (García-Aguilar et al., 2014, 2015; Palmqvist et al., 2022a), show that the quicksand acts as a trap for the animals caught. Espigares et al. (2023) proposed that this scenario would explain the high abundance of skeletal remains of megaherbivores, particularly elephants, in the UAL of FN3, and also the high density of hyena coprolites, because the half-sunken carcasses of the animals that regularly got stuck in the muddy sands would have attracted the scavenging hyenas.

Another way of fluidization for a quicksand can be vibrations from an earthquake (Kadau et al., 2009). Of interest here, paleo-seismites are frequently recorded in the Orce sediments and throughout the whole Baza Basin, which shows that this region was tectonically and seismically active during the Quaternary (Alfaro et al., 1997, 2010; García-Aguilar et al., 2014; Gibert et al., 2005). In fact, the dome-shaped surface of the limestone layers of FN3 can be interpreted as resulting from earthquakes (see Fig. 3).

Most research on quicksand focuses on the danger it poses to man-made structures (Craig, 1997; Elbaz et al., 2016; Sun, 2016; Xu et al., 2009). However, with the only exception of Hungerbühler (1998), who proposed a quicksand-like trap as an explanation for the finding of 17 partial skeletons of the Late Triassic prosauropod dinosaur *Sellosaurus gracilis,* as far as we know no paleo-quicksand has been reliably identified in the sedimentological record. For this reason, it is of great interest to test if layer 5 of the UAL of FN3 could have behaved as a quicksand in which very large animals became entrapped, as proposed by Espigares et al. (2023).

1.3 Objectives

The two main goals of this study are: (i) to test for statistical differences in the composition of the fossil assemblages of large mammals preserved in the LAL and UAL of FN3; and (ii) to analyze particle size in the main fertile layers of the LAL (layers 2–3) and UAL (layer 5), which preserve most skeletal remains of large mammals unearthed from the FN3 site, in order to test the hypothesis of entrapment of megaherbivores in quicksand proposed by Espigares et al. (2023) for layer 5 of the UAL.

2 Material and methods

Published data on the composition of the vertebrate assemblages unearthed from the two main archaeological levels of the FN3 site were compiled from Espigares et al., (2019: Tables S7-S8) for the excavation seasons of the years 1999–2015, and from Yravedra et al., (2021: Table 1) for those performed during the years 2017–2020. Species abundances were recorded as numbers of identifiable specimens (NISP) and estimates of minimum numbers of individuals (MNI). The latter were distributed among two major age categories, juveniles with milk teeth and adults with permanent dentition. Statistical comparison between the frequencies of taxa and size/age categories in the LAL and UAL were based on the z-test (Lawley, 1938).

Three samples of sediment were taken from the FN3 site for analyzing particle size. One sample is from layer 5 of the UAL, which is homogeneous in grain size, color and texture (Fig. 2B–C). As indicated above, this layer preserves a huge accumulation of skeletal remains of megaherbivores and hyena coprolites (see Espigares et al., 2023). The other two samples are from layers 2–3 of the LAL, in which other herbivores are comparatively more abundant and manuports are better represented. Of the latter samples, the first corresponds to the bottom of layer 2, which sediment shows a light tone (Fig. 2C), and is hereafter referred to as sample 2. The second sample was taken at the top of layer 2, which has a darker tone. Given that the upper part of layer 2 shows an irregular bedding surface due to soft-sediment deformation (Fig. 2C), the sample also includes sediments from the bottom of layer 3. For this reason, this sample is hereafter referred to as sample 3.

Part of the sediment contents of the three samples studied were washed using 0.710 mm, 0.500 mm and 0.125-mm mesh sieves. After drying the fractions recovered, an Olympus SZH-10 binocular magnifier was used in order to recognize ostracod and mollusk remains. Scanning Electron Microscopy (SEM) images of microfauna were taken using a JEOL JSM-6490LV device from 'Servicios Centrales de Apoyo a la Investigación' (SCAI, University of Málaga, Spain), equipped with W filament.

Particle size was also measured in the samples by sieving and laser diffraction. In this case, sieve aperture ranged from -1ϕ to 4ϕ. Larger sieve sizes were omitted due to the huge amount of sample that would have been required to ensure a representative analysis. Particle size analysis of the silt and clay fractions was performed using a Beckman Coulter LS13 320 Laser Diffraction Particle Size Analyzer. Particles were classified among size classes following Blott and Pye (2012) and data were analyzed using a custom GRADISTAT sheet (Blott & Pye, 2001), modified to calculate the porosity following the formula of Wu and Wang (2006). These analyses were performed at the Geology Laboratory of 'Centro Nacional de Investigación de la Evolución Humana' (CENIEH, Burgos, Spain).

3 Results

3.1 Differences between the large mammal assemblages of the LAL and UAL

Table 1 shows data on the composition of the bone assemblages unearthed from FN3, distributed among archaeological levels and excavation seasons. According to this information, the abundance of skeletal remains of megaherbivores (i.e., those species with an adult body mass of > 1000 kg, including elephant *M. meridionalis,* hippo *H. antiquus* and rhino *S. hundsheimensis*) relative to other large mammals (i.e., those species weighing > 5 kg) is higher in the UAL than in the LAL. Specifically, megaherbivores represent 63.9% (1060/1658) of the NISP of large mammals in the UAL and only 17.0% (105/616) in the LAL. A z-test (Lawley, 1938) shows that this difference in frequencies is statistically highly significant ($z = 19.879$, $p < 0.00001$). Similarly, megaherbivores account for 32.6% (28/86) of the MNI calculated for the large mammals in the UAL and for only 11.8% (6/51) in the LAL. This difference is also statistically significant, albeit to a lesser degree ($z = 2.724$, $p = 0.0065$) given that the MNI estimates are lower than the NISP counts. These data unequivocally confirm that the frequency of megaherbivores is about three times higher in the UAL than in the LAL, as previously suggested by Espigares et al., (2019, 2023).

Concerning the distribution of MNI estimates among age classes [Table 1, data based only on Espigares et al. (2019); Yravedra et al. (2021) did not provide this information separately for each archaeological level], megaherbivores are represented in the UAL by a higher MNI of juvenile individuals, 58.8% (10/17), than other ungulates, 23.3% (7/30), which is a significant difference ($z = 2.433$, $p = 0.0151$). In the LAL, however, the frequency of juvenile megaherbivores, 50% (2/4), and the proportion of non-adults in other ungulate species, 28.1% (9/32), do not differ significantly ($z = 0.895$, $p = 0.\ 3681$), which is due to the low sample size of megaherbivores in this archaeological level. In which concerns the relative abundance of age classes for ungulates other than megaherbivores, the frequencies of juveniles (23.3% in the UAL and 28.1% in the LAL) are similar in both archaeological levels ($z = 0.431$, $p = 0.6672$).

Table 1 also shows that the frequency of horses (*E. altidens, E. suessenbornensis* and *Equus* sp.) relative to other herbivores in the LAL, 62.9% (378/601) according to NISP counts and 46.7% (21/45) based on MNI estimates, is higher than in the UAL, 17.6% (281/1593) and 22.2% (16/72), respectively. These differences in frequencies are both statistically significant ($z = 20.622$, $p < 0.00001$ and $z = 2.766$, $p = 0.0056$, respectively).

Finally, the frequency of carnivorans (all adults) in the fossil assemblage of large mammals does not differ between the LAL and UAL based on NISP counts, 2.4% (15/616) and 3.9% (65/1670), respectively ($z = 1.682$, $p = 0.0929$), and neither according to MNI estimates, 11.8% (6/51) and 16.3% (14/86), respectively ($z = 0.723$, $p = 0.4715$).

Therefore, our results show that megaherbivores are comparatively overrepresented in the UAL, particularly by young elephants, while other ungulates (especially equids) are more abundant in the LAL, showing a predominance of adult individuals. Moreover, Espigares et al., (2023: Table 1) showed that most hyena coprolites preserved in FN3 come from the UAL (98.6%, 217 out of 220), while most manuports are from the LAL (87.7%, 329 out of 375) (see Fig. 4). Both differences are statistically highly significant ($z = 20.404$, $p < 0.00001$ for coprolites; $z = 20.667$, $p < 0.00001$ for manuports), which suggests that different site formation processes were involved in the two main archaeological levels of FN3.

3.2 Differences of grain size composition between the fertile layers of the LAL and UAL

There is a clear difference in grain size between layer 5 of the UAL, which shows a predominance of sands, and layers 2–3 of the LAL, in which fine-grained particles predominate (Fig. 5, Table 2). Specifically, layer 5 shows an elevated proportion of fine and very fine sands (64.4%), with a mode at 94 µm, a very low frequency of medium, coarse, and very coarse sands (only 2.5%), and a moderate proportion of silt and clay (33.1%). In the case of samples 2–3, fine and very fine sands represent lower fractions (12.9% and 18.5%, respectively) than in layer 5, while silts and clays show much higher frequencies (84.9% and 79.4%, respectively). According to the grain size distribution of Table 2, fine silts are represented by a higher proportion in layer 2 than in layer 3, with a mode at 6 µm, and clay contents (29.5%) are also more abundant. In contrast, layer 3 has more fine sands and coarse silts, with modes at 187.5 and 24 µm, respectively, and somewhat lower clay contents (21.2%). These results show that the overall particle size distribution of sample 3 shows some similarities with that of layer 5, although it has much lower sand contents and a remarkably higher frequency of very fine-grained sediments.

3.3 Differences between the ostracod and mollusk assemblages of the LAL and UAL

The stratigraphic section of FN3 not only shows significant differences in lithology and granulometry, but also in the invertebrate contents of the fertile layers of the LAL and UAL. Layers 2–3 of the LAL show differences in the composition of their ostracod and mollusk assemblages. Specifically, layer 2 preserves shells of the ostracods *Ilyocypris bradyi* and *I. gibba* (Fig. 6A), as described by Anadón et al. (2003) in a study based on a more extensive sampling of this layer. Moreover, Anadón et al. (2003) also identified in this layer the presence of the ostracod *Candona angulata*. Shells of *I. bradyi* and *I. gibba* are also found in layer 3, as well as scarce remains of the ostracod *Heterocypris incongruens* (Fig. 6B). In contrast, the UAL shows a predominance of the ostracod *Cyprideis torosa,* which is represented by both smooth and node-reticulated valves (Fig. 6C). The latter valves are less abundant, at least as far as layer 5 is concerned. Anadón et al. (2003) also highlighted the presence in several stratigraphic layers of FN3 of the ostracods *Heterocypris salina* and *Ilyocypris* sp., as well as operculum remains of the freshwater snail *Bithynia* sp., which are recorded in low frequencies. Our study shows that these remains are associated in layer 5 to shell accumulations of the land snail *Limax* sp. (Fig. 6D).

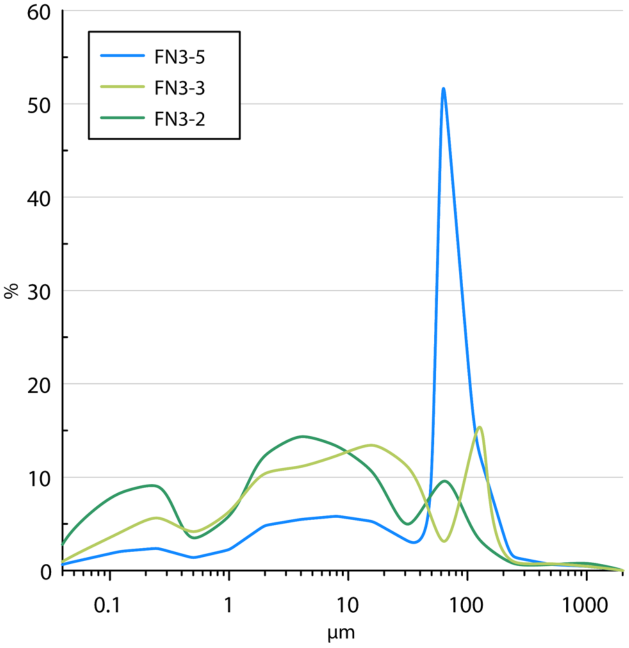

Fig. 5 Particle size distribution of the sedimentary samples of the late Early Pleistocene site of Fuente Nueva-3 (FN3) analyzed in this study (data from Table 2). Sample 5 is from layer 5 of the upper archaeological level (UAL). Samples 2–3 are from the lower archaeological level (LAL). Specifically, sample 2 was taken at the bottom of layer 2, which sediments show a light tone, while sample 3 is from the top of layer 2, which sediments show a dark tone, and from the bottom of layer 3

4 Discussion

Espigares et al. (2023) suggested that the lithological differences between the LAL and UAL, the two main archaeological levels of FN3, could explain the differences in

Table 2 Particle size analysis of three selected stratigraphic layers of FN3. Statistical values calculated by GRADISTAT (Blott & Pye, 2001)

	Aperture (µm)	FN3-2	FN3-3	FN3-5
		Class weight retained (%)	Class weight retained (%)	Class weight retained (%)
Clay	0.04	2.79	0.95	0.63
	0.125	8.35	4.14	2.05
	0.25	9.01	5.62	2.35
	0.5	3.5	4.17	1.39
	1	5.86	6.32	2.26
Silt	2	12.3	10.38	4.79
	4	14.33	11.14	5.47
	8	13.32	12.3	5.8
	16	10.49	13.41	5.22
	32	4.98	10.99	3.13
Very fine sands	63	9.56	3.13	51.64
Fine sands	125	3.37	15.34	12.72
Medium sands	250	0.72	0.9	1.43
Coarse sands	500	0.64	0.72	0.66
Very coarse sands	1000	0.76	0.45	0.44
Gravel	2000	0	0	0
	Mode 1 (µm):	6	187.50	94
	Mode 2 (µm):	94	24	-
	Mode 3 (µm):	0.375	0.375	-
	D_{10}:	0.23	0.46	2.42
	D_{50}:	5.944	12.04	78.84
	D_{60}:	9.77	20.67	90.01
	D_{90}:	90.49	174.70	166.42
	Clay (%)	29.51	21.20	8.60
	C_u	43.04	45.13	37.19
	Porosity (%)	70.97	64.43	48.61

Porosity calculated after Wu and Wang (2006)

composition between their bone assemblages of large mammals. Specifically, layers 2–3, the two fossiliferous layers of the LAL, are composed of green clays (layer 2) and brown-whitish clays with nodules (layer 3). In contrast, layer 5, which preserves most skeletal remains of the UAL, is composed of fine greenish sands (the greenish tone probably results from the clay contents of this layer) and marly mudstones (see also Oms et al., 2011). For this reason, Espigares et al. (2023) proposed that the sediments of layer 5, which are mostly represented by fine sands and clays, (i) may have behaved like quicksand that became unstable when forced to move by the pressure exerted by very large ungulates; and (ii) the entrapped carcasses of these large-sized animals lured scavenging carnivores like the hyenas and hominins. In the case of hyenas, they regularly visited the site during this time interval and defecated in the surroundings of the carcasses of megafauna on which they fed, thus giving rise to a latrine of *P. brevirostris* in an open-air setting (Espigares et al., 2023).

Our statistical comparison of the bone assemblages preserved in the LAL and UAL of FN3 shows that the abundance of megaherbivores relative to other large mammals is between 2.8 and 3.7 times higher in layer 5 than in layers 2–3, depending on whether the comparison is based on MNI estimates or NISP counts (Table 1), respectively. In addition, megaherbivores are represented in layer 5 by juveniles in a proportion 2.5 times higher than that calculated for other ungulates.

Our grain size analysis (Fig. 5, Table 2) confirms that layer 5 of the UAL shows a predominance of very fine and fine sands, which account for nearly two-thirds of the sediments that make up this layer, and that silt and clay represent most of the remaining fraction. In contrast, layers 2–3 of the LAL are mainly composed of silt and clay, showing < 20% of sand contents. All these data tentatively support the hypothesis of Espigares et al. (2023) that layer 5 of FN3 could have represented a death trap for megafauna in quicksand.

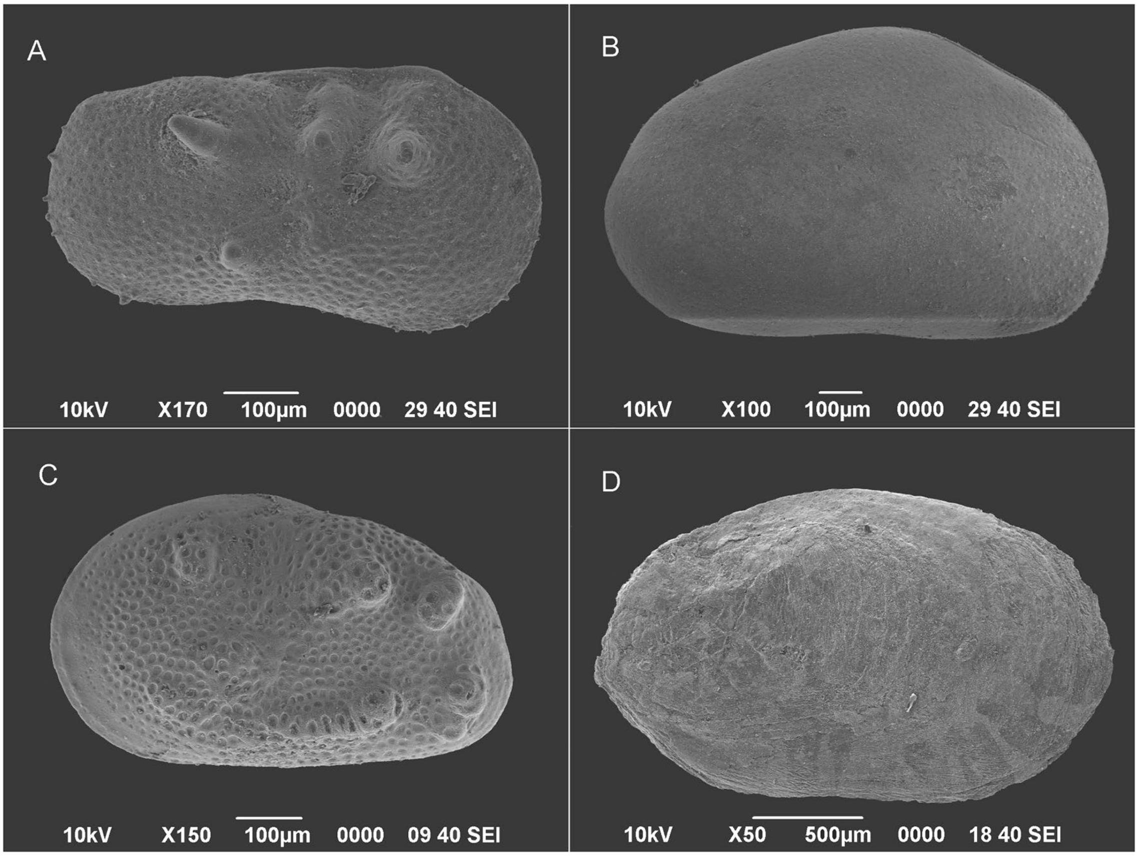

Fig. 6 SEM photographs of shell remains from the late Early Pleistocene site of Fuente Nueva-3 (FN3). **A** Right valve of the ostracod *Ilyocypris gibba*. **B** Right valve of the ostracod *Heterocypris incongruens*. **C** Left node-reticulated valve of the ostracod *Cyprideis torosa*. **D** Shell of the pulmonate gastropod *Limax* sp.

The micropaleontological contents of the fossiliferous layers indicate that the faunal assemblage of layers 2–3 of the LAL consists of ostracods that lived in a permanent lacustrine environment with ephemeral fresh to oligosaline waters (Anadón et al., 2015; Fuhrmann, 2012; Granados et al., 2021). In contrast, layer 5 of the UAL shows a predominance of species indicative of a brackish lacustrine environment, as evidenced by the presence of *C. torosa* with smooth valves (Fig. 6C) (see Anadón et al., 1994; Granados et al., 2021). The finding of a low frequency of shells of this species showing nodose valves would indicate occasional reductions of salinity in the environment (Anadón et al., 2015; Fuhrmann, 2012). In addition, the presence of *Ilyocypris* sp. (reported in Anadón et al., 2003) is probably indicative of fluvial inputs from a nearby spring (Fuhrmann, 2012), while the presence of the land snail *Limax* sp. suggests the subaerial emersion of these sediments. Therefore, compared to the situation depicted in layers 2–3 of the LAL, the mixture of faunas and the shell concentrations of *Limax* sp. in the UAL suggest a periodic drop of the lake waters, which would led to occasional emersions. This would imply that the sediments of the UAL remained saturated in water with moderate to high salinity, as particularly evidenced in the case of layer 5, which is relevant for our interpretation of this layer as a potential quicksand trap for megaherbivores, as discussed below.

4.1 The upper archaeological level of FN3 as a natural trap for megaherbivores

As noted before, experimental data on quicksand composed of fine sand, clay and salt water from salt-lake environments similar to the oligosaline lacustrine systems of the Baza Basin (García-Aguilar et al., 2014, 2015; Palmqvist et al., 2022a) show that the quicksand can trap animals wandering on its surface. However, the objects with a density of 1 g/ml (i.e., the average density of mammalian tissues) are not completely sucked beneath the surface but sink halfway into the quicksand (Khaldoun et al., 2005, 2006). Therefore, a quicksand scenario would explain the entrapment of megaherbivores in the UAL of FN3 and the high numbers of coprolites unearthed from this archaeological level (Fig. 4), because the partly sunk carcasses of very large animals that regularly became entrapped in the muddy sands of layer 5 would have attracted the hyenas, which fed on these carcasses and defecated in their surroundings (Espigares et al., 2023).

Whether or not a given sandy sediment behaves like a quicksand depends on its lithology (e.g., granulometry and sand composition) and also on a number of factors (e.g., seismic movements, porosity, water saturation, water salinity, and pressure) of which some do not fossilize. Given these constraints, the interpretation of a paleo-quicksand relies on sedimentological data but must also be corroborated by other sources of evidence, including taphonomic and tectonic factors. According to current studies on quicksand (SUCTC, 2012; Gao et al., 2018), a substrate should show the following properties for considering it as a potential quicksand: (i) a predominance of fine sands and silts; (ii) a clay-size fraction of < 10%; (iii) a thickness of > 0.25 m; (iv) a coefficient of uniformity of < 5; (v) a porosity of > 43%; (vi) water contents of > 30%; (vii) a soil in a saturated state; and (viii) a low permeability and poor drainage.

The clay-size fractions of samples from layers 2–3 of the LAL (Fig. 5, Table 2) are well above the limit (10%) for classifying them as quicksand. In contrast, the sample from layer 5 of the UAL shows a low clay content of < 10%, being primarily composed of fine and very fine sands. Therefore, this layer satisfies the first and second constraints, being a good candidate to be considered as a potential paleo-quicksand.

Layer 5 shows an uneven thickness due to the erosion and levelling of the irregular top of layer 4 (Espigares et al., 2023; Oms et al., 2011), and is affected by soft-sediment deformation (Fig. 2B–C). After ~ 1.4 Ma of diagenetic compaction, layer 5 ranges in thickness between 10 and 30 cm. Considering the porosity calculated for this layer (48.6%; see Table 2), it would be expected that the original thickness was at least 25% greater (Lundegard, 1992), an estimate that would satisfy the requirement of a sediment thickness of > 25 cm over most of the lateral extent of layer 5.

The coefficient of uniformity (determined by the ratio D10:D60) calculated for the sample from layer 5 (37.2) is higher than the maximum limit for a quicksand, which is set at 5. Layer 5 primarily consists of fine sands showing a mode of 94 µm (Table 2). These sands were deposited by a low-energy flow, as evidenced by the erosive bottom of layer 5 and the lenticular shape observed in the stratigraphic section (Fig. 2). Layer 5 also has a silt and clay fraction in excess of that expected for a quicksand.

In a recent study, Yravedra et al. (2024) indicate the presence in layer 5 of five sublayers with different microfacies, of which some show a predominance of sands while others are rich in silts and clays. Specifically, the silt and clay fraction identified in our study of a sample of sediment from layer 5 (Table 2) could correspond to the basal sublayer and upper sublayers described by Yravedra et al. (2024) in this stratigraphic level, which they characterize as sandy clays and mudstones (microfacies 1, 4 and 5 of Yravedra et al., 2024). In contrast, our fraction of fine sands in the sample from layer 5 could correspond to the mostly sandy sublayers located immediately below a partial skeleton of the proboscidean *M. meridionalis* (microfacies 2 and 3 of Yravedra et al., 2024). In this way, the coefficient of uniformity of these sandy sublayers with low silt and clay contents would be compatible with a quicksand.

Another possible explanation for the presence of fine-grained sediments in layer 5 is that they could have entered in this layer after the original accumulation of the deposit, which was followed by soft-sediment deformation and diagenesis. In fact, layer 6 consists of mudstones (Oms et al., 2011) and has similar characteristics to layer 3, with analogous proportions of silts and clays. This opens the possibility that the finest sediments of layer 5 come from layer 6, the overlying stratum, by edaphic processes that lixiviated the fine-grained sediments of layer 6 and percolated them into layer 5. In addition, the silts and clays of layer 5 (Fig. 5; Table 2) are consistent with the grain size distribution of the global aeolian dust (Lawrence & Neff, 2009), which means that aeolian transport cannot be ruled out as a source of sediment. Of interest here, the Iberian Peninsula continuously receives African dust, which is deposited in the Mediterranean soils (Bout-Roumazeilles et al., 2007; Escudero et al., 2011). Loess deposits consisting of coarse and fine silts and clays have been identified in the Granada Basin from the Pliocene to the present (Günster et al., 2001; Wagner et al., 2015). Therefore, we can assume that aeolian sediments were also deposited on the surface of layer 5, which would also potentially account for the most fine-grained fraction of this layer.

Post-depositional processes such as pedogenesis and diagenesis are another potential source of fine-grained sediments. Primary soil-forming mechanisms for Mediterranean soils include clay illuviation, carbonate redistribution and aeolian inputs (Yaalon, 1997). These processes, coupled with the weathering of siliciclastic sediments, generate fine-grained sediments. In fact, the pedogenetic processes observed in the Granada Basin result in an increase in the abundance of fine-grained sediments at the expense of the coarser fraction (Günster et al., 2001; Wagner et al., 2015). Sand diagenesis can lead to mineral compaction, dissolution and reprecipitation, which results in a decrease in particle size distribution as smaller minerals are precipitated replacing the original ones (Marfil & De la Peña, 1989). These processes would increase the proportion of fine-grained sediments in layer 5 after the burial of the stratum. If we tentatively assume that there were no fine-grained sediments during the subaerial exposure of layer 5, the coefficient of uniformity of the sand would then be 1.59, a value in agreement with the limit of < 5 required for a quicksand.

Porosity was calculated assuming a unimodal distribution. Layer 5 is near to unimodal distribution, with a mode in 94 µm and a porosity of 48.6% (Fig. 5, Table 2). If the silt and clay fractions are considered, porosity may vary to some degree. However, the finest sediments may have been generated later due to pedogenetic and diagenetic processes, as discussed before.

The ostracod assemblage of layer 5 suggests oligosaline conditions in the lake waters, with periodic variations of salinity over time. The shells of *C. torosa* are indicative of a shallow lacustrine environment near a coastal zone (Anadón et al., 1994; Granados et al., 2021), which was influenced by the arrival of fine-grained detrital sediments. These inputs of freshwaters are evidenced by the presence of *Ilyocypris.* The shell accumulations of terrestrial gastropod *Limax* sp. indicate periods of subaerial exposure in this area, which would have allowed the transit of megafauna and their predators from the surrounding environments. Therefore, the sediments of layer 5 in the UAL were likely influenced by brackish waters, which salt contents favored the development of a quicksand trap, as evidenced by the experiments of Khaldoun et al. (2005).

The constraints related to water contents and permeability [i.e., those addressed above in points (vi), (vii) and (viii)] are not recorded in the stratigraphic sequence, but they can be inferred from the paleoenvironment of FN3, which is interpreted as a lake margin subject to small, low-energy flows. This lake may have experienced periods of flooding and recession, which would cause the lake margin to become a water-saturated soil, in agreement with the environmental reconstruction of Espigares et al., (2013, 2019), Yravedra et al., (2021, 2024) and Palmqvist et al. (2023a). Layer 4 is a limestone bed (Espigares et al., 2023; Oms et al., 2011) and these limestones may have acted as a low permeability layer, which may have eventually led to a poor drainage of layer 5. Thus, it is likely that layer 5 became saturated with oligosaline waters due to insufficient drainage, which satisfies conditions (vi), (vii) and (viii).

In summary, both the sedimentological data and the paleoenvironmental reconstruction of layer 5 indicate that it may be interpreted as a paleo-quicksand deposit that may have functioned under certain conditions as a natural trap for very large animals, which would explain the high frequency of megaherbivores recorded at the UAL of FN3.

4.2 Entrapment of megaherbivores in the upper archaeological level of FN3

Mud entrapment is a relatively common phenomenon today in Africa, because elephants and other large mammals venture during drought episodes into drying dams in their quest for drinking water and taking mud baths. Giant naked-skinned animals such as elephants, rhinoceroses and hippos usually wallow in mud to thermoregulate and protect themselves from insect bites and parasites. However, their huge size poses a risk of being mired in the mud. Figure 7 depicts one of these entrapment events, in which a mother elephant and her calf became stuck in a muddy waterhole during the height of the 2019 dry season in Mana Pools National Park, Zimbabwe. Eventually, the calf was eaten alive by a pack of spotted hyenas (*Crocuta crocuta*) and the mother succumbed days later, probably due to dehydration.

Increased exposure of megaherbivores to the risk of entrapment in quicksand results from the high weight per unit area supported by their limbs. Given that the three species of megaherbivores recorded at FN3 are extinct, there are no direct measurements on the ground support surface of their feet. However, reliable estimates can be retrieved from their modern analogues and also from fossil footprints (although it should be noted that footprint dimensions can overestimate or underestimate the actual foot dimensions; for review and references, see Masao et al., 2016).

In the case of elephant *Mammuthus meridionalis,* Pasenko (2017) provided useful data on body mass and footprint diameters of the forefeet and hindfeet for a number of extant African (*Loxodonta africana*) and Asian (*Elephas maximus*) elephants, which are useful for estimating the weight per unit area supported by their feet. For example, the average footprint length and width of the manus (forefoot), 48.5 × 38 cm, and pes (hindfoot), 47 × 30 cm, of an adult male of *L. africana* of 4899 kg allow estimating the area of the footprint ellipses of its manus (1432.6 cm^2) and pes (1083.9 cm^2), which results in a ground support surface for all four feet of 5033 cm^2. Considering the body mass of this individual, the weight per unit area supported by its feet would be 0.97 kg/cm^2. Following this procedure, an adult female of *E. maximus* of 3962 kg shows average length and width diameters of the manus (42 × 38 cm) and pes (39 × 28 cm) that result in a ground support surface for all four feet of 4180.4 cm^2, which provides a similar estimate of weight per unit area, 0.95 kg/m^2. In a five-years old male of *L. africana* of 1515 kg, the manus and pes diameters (34.5 × 24.5 cm and 35 × 21 cm, respectively) allow estimating a ground support surface for all four feet of 2350 cm^2, which results in a lower weight per unit area, 0.64 kg/m^2. Finally, the manus (31 × 22.5 cm) and pes (29.5 × 19.5 cm) diameters of the footprints of a 1.5-years juvenile male of *L. africana* of 726 kg translate in a ground support surface for all four feet of 1929.7 cm^2, which corresponds to a weight per unit area of only 0.38 kg/m^2. These measurements of footprints for extant elephants agree with those reported by Altamura et al. (2023) for fossil footprints produced by young and adult individuals of the straight-tusked elephant *Palaeoloxodon antiquus* in the Middle Pleistocene site of Schöningen (Germany), dated to ~ 321 ka, and also with the footprint tracks of this species described by Neto de Carvalho et al. (2021) in the Late

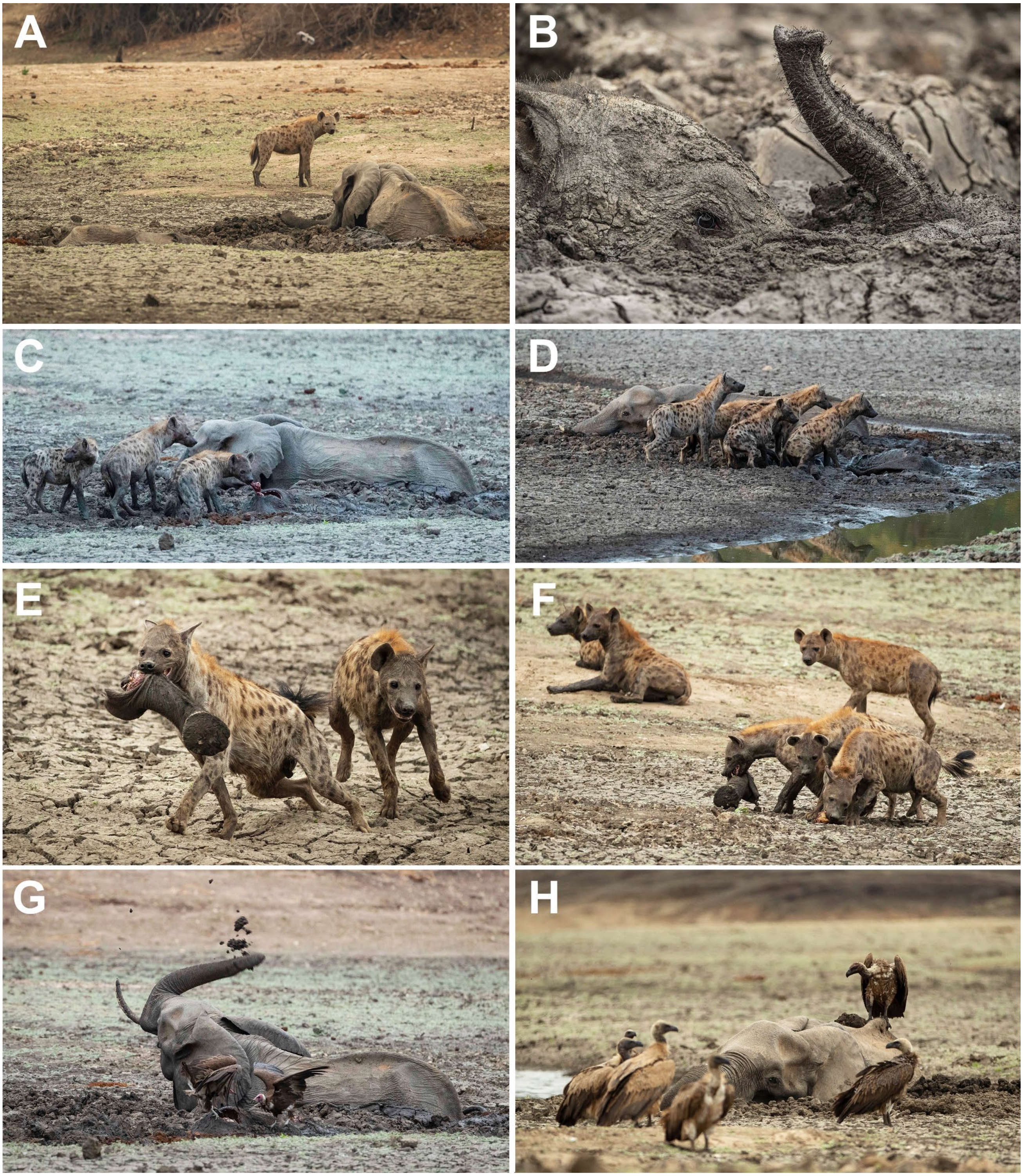

Fig. 7 Two elephants (*Loxodonta africana*), mother and calf, got stuck in the mud while searching for water during the 2019 dry season in Mana Pools Natural Park, Zimbabwe. Soon after, spotted hyenas (*Crocuta crocuta*) came and roamed around them (**A**). The calf, which could barely breathe by sticking its trunk out of the mud (**B**), was eaten alive that night to the helplessness of its mother (**C**). The hyenas fed on the carcass until the next morning (**D**), dismembered it (**E**) and carried the limbs to be consumed at a distance (**F**). The vultures (hooded vulture, *Necrosyrtes monachus,* in **G**; white-backed vulture, *Gyps africanus,* in **H**) fed on the remains of the calf carcass while the mother elephant tried to chase them away by throwing mud (**G**). Finally, the vultures landed on the mother's body, waiting for her death (**H**). The adult elephant was rescued from the mud with a crane but did not survive stress and dehydration. Montage made by the authors with photographs taken by Jens Cullmann (https://jenscullmann.de), reproduced with permission of the author

Pleistocene (MIS 5) site known as the Matalascañas Trampled Surface in Huelva (Spain). In the latter site, 34 footprints attributed to newborns, calves, juveniles, and adults were measured (Neto de Carvalho et al., 2021: Table 1). The length and width diameters of these footprints range between 9.6 × 7.6 cm in calves of < 1 year and 54.5 × 31.6 cm in adults of > 60 years, values that are similar to those measured in extant elephants. If we consider the body masses calculated for these specimens by Neto de Carvalho et al. (2021), the estimates of ground support surface for all four feet would be comprised between 0.24 kg/m^2 in calves and 1.03 kg/m^2 in old adults, respectively.

In the case of the giant, short-limbed *Hippopotamus antiquus* (Palmqvist et al., 2022b), Behrensmeyer and Laporte (1981) reported on the finding of single footprints and trails of large vertebrates in a 12 cm thick unit of sandy muds (sand:silt:clay = 12:59:29), dated to 1.6–1.5 Ma and deposited in a marginal lacustrine environment of the Koobi Fora Formation (Kenia). Among these footprints, there are several deep, four-toed impressions of hippopotamus feet and a shallow depression resembling a human footprint. According to Behrensmeyer and Laporte (1981), the larger footprints (25–32 cm wide on average) can be attributed to the giant *Hippopotamus gorgops,* a huge extinct sister species with a size and anatomy similar to *H. antiquus* (~ 3200 kg; Palmqvist et al., 2022b), while the smaller ones (18–20 cm wide) may be from juveniles of this species or even belong to the fossil pigmy species, aff. *Hippopotamus aethiopicus* (Boisserie, 2005). The larger footprints, each describing an ellipse with an area of 628.3 cm^2, result in a minimum ground support surface for all four feet of 2513.2 cm^2. Given the mass of *H. gorgops,* this would provide a weight per unit area of 1.27 kg/cm^2. Similarly, Bennet et al. (2014: Fig. 9D) figured one footprint attributed to *H. gorgops* from an ichnological surface close to Koobi Fora (GaJi10), which is dated to 1.4 Ma (Bennett et al., 2014). The digitization of this footprint with ImageJ software provided an area of 814 cm^2, which allows estimating a ground support surface for all four feet of 3256 cm^2. This would in turn result in a weight per unit area of 0.98 kg/cm^2. In contrast to *H. gorgops,* the weight per unit area is lower in the living *H. amphibius,* almost half of the estimate obtained for the giant, short-limbed extinct hippo. Specifically, Altamura et al. (2017) published a tracksite presumably made by *H. amphibius* in the Middle Pleistocene site of Gombore II-2 (Melka Kunture, Upper Awash, Ethiopia), which is dated to ~ 0.7 Ma (Altamura et al., 2018). Digitization with ImageJ of the best-preserved footprint (Altamura et al., 2017: Fig. 8B) provided an area of 693 cm^2, which results in a ground support surface for all four feet of 2772 cm^2. Given that the body mass of the modern common hippo (~ 1420 kg; Palmqvist et al., 2022b) is less than half that estimated for *H. antiquus,* this would translate in a weight per unit area of only 0.51 kg/cm^2, which would represent a lower risk of entrapment for the living hippo compared to the giant extinct hippo.

Concerning the extinct rhino *Stephanorhinus hundsheimensis,* Leakey and Hay (1979) provided average measurements for the forefoot and hindfoot footprints of two fossil rhinos, the black rhino *Diceros bicornis* (~ 1100 kg; Mendoza et al., 2006), and the white rhino *Ceratotherium simum* (~ 1600 kg; Mendoza et al., 2006). These fossil footprints are

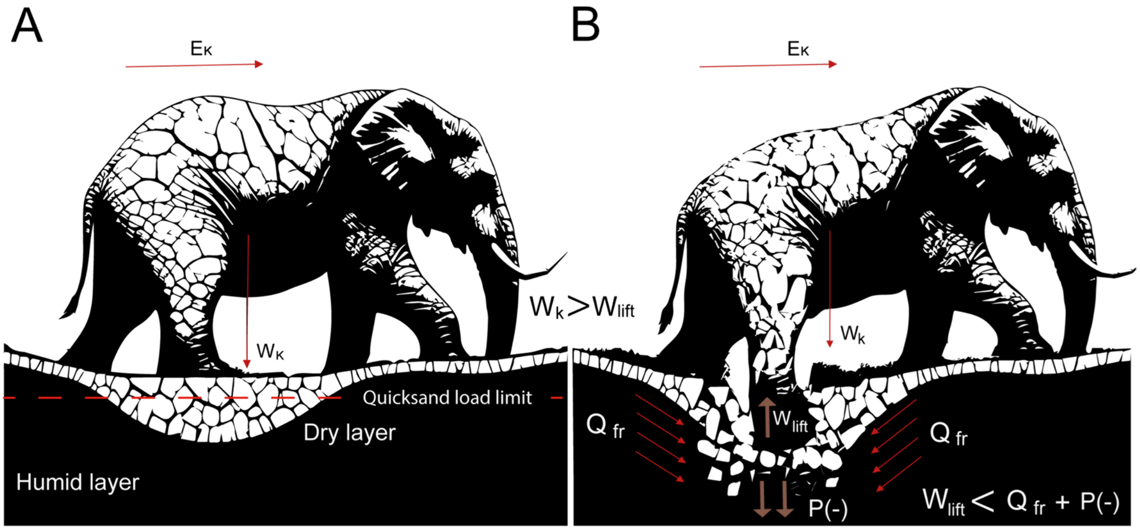

Fig. 8 Entrapment of an elephant in the quicksand of layer 5 of the upper archaeological level of the late Early Pleistocene site of Fuente Nueva-3. Abbreviations: E_k, kinetic energy; W_k, impact transfer work, in J; W_{lift}, mechanical work required for the upward thrust of the limbs, in J; Q_{fr}, friction coefficient; $P_{(-)}$, negative pressure. Elephant silhouettes were obtained with an AI image generator (https://chat.openai.com/g/g-tvADFu1PW-generador-de-imagenes). Figure composed and edited by A. Perez-Ramos using Adobe illustrator

Fig. 9 **A** Partial skeleton of an elephant (*Mammuthus meridionalis*) unearthed from layer 5 of the upper archaeological level of the late Early Pleistocene site of Fuente Nueva-3 (photograph taken by the authors). The age at death of this individual has been estimated at 55–60 years according to the wear of the third lower molar. The curvature of the jaw symphysis unequivocally indicates that it was a female individual (see Espigares et al., 2013). The mandible, vertebral column, ribs, and pelvis were all preserved in anatomical connection, although some ribs and vertebrae were slightly displaced by post-depositional processes. The elephant skeleton is partially surrounded by 34 hyena coprolites and 17 flakes. The tone of these coprolites, which are darker than other unearthed from layer 5, evidences that the hyenas consumed large amounts of the elephant's meat and fat. The coprolites and flakes partially overlap in their distribution, suggesting competition between the hominins and hyenas for the elephant carcass (see discussion in Espigares et al., 2013, 2023; Palmqvist et al., 2023a; for an opposite interpretation, see Yravedra et al., 2024). **B** Adult female elephant and her two young caught in a mud trap in Kenya (photograph taken by Kieran Avery, reproduced with permission of the Sheldrick Wildlife Trust)

preserved in the Late Pliocene Upper Laetolil Beds (Tanzania), which are dated to 3.85 – 3.63 Ma (Deino, 2010). In the case of the footprints attributed to *D. bicornis,* the average dimensions of the forefoot (24.6 × 24.8 cm) and hindfoot (25.6 × 22.8 cm) translate in a ground support surface for all four feet of 1734.2 cm^2, which results in a weight per unit area of 0.63 kg/cm^2. The larger trails, attributed by Leakey and Hay (1979) to *C. simum,* have average dimensions of the forefoot (28.5 × 31 cm) and hindfoot (40 × 27 cm) that allow estimating a ground support surface for all four feet of 3084.2 cm^2. These estimates would in turn result in a weight per unit area of 0.52 kg/cm^2. Footprint area values for modern black rhino in Mwabvi Game Reserve can be derived from average diameters of forefeet (23 cm) and hindfeet (19.7 cm) provided by Jachmann (2001: Table 10.1; the last individual track was excluded because it was probably made by a juvenile). These measurements allow estimating a ground support surface for all four feet of 1440.6 cm^2, which results in a weight per unit area of 0.76 kg/cm^2.

In summary, the elevated weight per unit area supported by the feet of the largest megaherbivores of FN3, which would fluctuate between 0.38 kg/cm^2 in the juvenile elephants and 1.27 kg/cm^2 in the adult giant hippos, would represent an increased risk of entrapment in quicksand compared to other ungulates of medium-to-large size.

In contrast to the megaherbivores, the weight per unit area supported by the feet of the two main scavenging carnivores at FN3, the giant hyena *Pachycrocuta brevirostris* and *Homo* sp. (Espigares et al., 2013, 2019; Palmqvist et al., 2011, 2023a), would be lower, which means a lower risk of being stuck in the quicksand. In the case of the hyena, the average size of the footprints measured by Leakey and Hay (1979) in four relatively long trails of the Laetolil Beds attributed to *Hyaena bellax* (a sister taxon of *P. brevirostris;* Palmqvist et al., 2011), 11.5 × 9.6 cm, translates in a support surface for all four feet of 442 cm^2. If we consider the body mass estimated for *P. brevirostris,* ~ 110 kg (Palmqvist et al., 2011), this results in a weight per unit area of 0.25 kg/cm^2. It is worth noting, however, that the European specimens of *P. brevirostris* show a larger size than their African counterparts, which means that their footprints were probably greater (and their weight per unit area lower) than these estimates. Concerning *Homo* sp., the dimensions (26 × 10 cm) of the human footprints of Koobi Fora reported by Behrensmeyer and Laporte (1981) allow estimating a ground support surface for the two feet of 408.4 cm^2. Considering a body mass of ~ 53 kg for *Homo* sp. in Orce (see Rodríguez-Gómez et al., 2016a, 2016b), this would result in a weight per unit area of only 0.13 kg/cm^2.

The above data refer to the weight per unit area supported by the feet of the animals under static conditions. However, the pressure exerted by the limbs increases when the animals are moving, depending on their speed. Specifically, the kinetic energy depends on the body mass (BM) of the animal and its velocity (v): $E_k = ½\ BM\ v^2$. Considering a moderate velocity of 3.07 m/s (Ren & Hutchinson, 2008) for the adult male of *L. africana* of 4899 kg cited before, this provides an E_k estimate of 23,086.3 J. This in turn results in an increase of pressure of 45,870 Pa. Given the ground support surface measured for all four feet in this specimen (5033 cm^2), this translates in an additional pressure of 0.47 kg/cm^2. If we sum this value to the static pressure, the weight per unit area supported by the elephant's feet under kinetic motion would be 1.44 kg/cm^2 (i.e. 50% higher than our previous estimate under static conditions). A speed of 5.56 m/s (20 km/h) would result in an increase of 1.53 kg/cm^2, which provides a weight per unit area of 2.5 kg/cm^2 (i.e., 1.5 times higher than the estimate for static conditions). Similarly, the increase of pressure for a speed of 3.07 m/s would be 0.612 kg/cm^2 in *H. antiquus,* which would result in a weight per unit area of ground support of 1.88 kg/cm^2. In contrast, the pressure under kinetic motion at this speed would rise in *P. brevirostris* and *Homo* sp. to 0.37 and 0.19 kg/cm^2, respectively, values that are both well below the penetration hardness of a quicksand (1–3 kg/cm^2 according to Nguyen et al., 2016: Fig. 6).

These data suggest that while adult megaherbivores, particularly elephants and hippos, could occasionally become trapped in the quicksand of layer 5 (Fig. 8), with the juveniles remaining in the vicinity of their mothers, the hyenas and hominins would have been much less exposed to this risk. For this reason, they could have scavenged the half-sunken carcasses of the megaherbivores that became stuck in quicksand. Interestingly, this is documented by a partial skeleton of an old female elephant in the UAL of FN3 (Fig. 9A). The skeleton preserves the mandible, vertebral column, ribs, and pelvis in anatomical connection, and is partly surrounded by flakes and hyena coprolites (Espigares et al., 2013, 2023). A similar scenario has been described for the remains of a Late Pleistocene American proboscidean (*Mammut americanum*) preserved in peaty silt and clay underlying till in a gypsum karst near Hillsborough, New Brunswick (Harington el al., 1993). In this case, nearly all of the postcranial elements on the right side of the body were preserved, whereas much the bones from the left side were missing or broken, except for the teeth and tusks. This suggests that this megaherbivore eventually sank deeply into the mud on its right side, leaving its exposed left side to be destroyed by the scavengers (Harington el al., 1993).

4.3 Hyenas and hominins in the upper archaeological level of FN3

As noted before, fossil remains of large mammals and lithic tools are abundantly preserved in layers 2–3 of the LAL and layer 5 of the UAL (Fig. 4). Moreover, although cut marks are relatively scarce, they are equally represented in the LAL and UAL (Espigares et al., 2019: Table S12). However, manuports are more abundantly recorded in the LAL, while hyena coprolites and skeletal remains of megaherbivores, particularly elephants, are concentrated in the UAL (Espigares et al., 2023: Table 1). Carnivorans tooth marks also predominate in this archaeological level (Yravedra et al., 2021: Table 5). These data suggest that although there is evidence in support of the involvement of hominins and hyenas in both archaeological levels, hominins exploited more intensively the resources available at the LAL, while hyenas concentrated their activity on the carcasses of megafauna at the UAL, for which sedimentological evidence suggests a quicksand trap as the most plausible sedimentary environment. In fact, the high frequency of coprolites in the UAL evidences that this area was frequently occupied by the hyenas during the period of time in which the UAL was formed. This suggests a partial ecological segregation between hyenas, which had more nocturnal and twilight habits, and hominins, who were predominantly diurnal.

Three scenarios have been discussed for carcass acquisition by the FN3 hominins (see review in Palmqvist et al., 2023a): (i) that the hominins had primary access to ungulate carcasses by hunting prey on their own; (ii) that they had early access to the prey of sabertooth cats and other primary predators after engaging them in confrontational scavenging (i.e., kleptoparasitism); or (iii) that they were able to locate the carcasses of animals dead by various causes (including predation) before other scavengers did.

No direct method allows to test if early *Homo* had primary access to ungulate carcasses by hunting or by early scavenging (Potts, 1991). However, the limited technological skills of the FN3 hominins make it difficult to argue that they could have hunted medium-to-large, large and very large prey on a regular basis: the small size of the flint flakes unearthed from FN3, few centimeters in most cases (Turq et al., 1996; Martínez-Navarro et al., 1997; Toro-Moyano et al., 2011; Espigares et al., 2013, 2019), suggests the lack of an effective weaponry for killing large ungulate prey (Palmqvist et al., 2023a), which makes it difficult to conceive how these hominins could have had a direct impact on megafauna hunting large-sized animals on their own (for a review on the ecology of Oldowan hominin carnivorous activity, see Blumenshine & Pobiner, 2007).

The second scenario, confrontational scavenging, is also unlikely because it would be dangerous for the hominins (Treves & Palmqvist, 2007). However, it must be noted that modern African agro-pastoralists successfully use rudimentary weapons like simple stones or long sticks to drive away lions, leopards and cheetahs from their kills and steal them (Treves & Naughton-Treeves, 1999). Moreover, it has been suggested that stone-throwing was an early adaptive strategy of *Homo,* which would explain the huge number of allochthonous cobbles found in the Early Pleistocene site of Dmanisi (Coil et al., 2020; Lordkipanidze, 2015). In the case of FN3, bone remains are also intermingled with abundant limestone cobbles (manuports), particularly in the LAL, in which hyena coprolites are very scarce (Fig. 4). This opens the possibility that the hominins transported the cobbles to the site and used them as weapons (i.e., as “flying stones”) for forcing predators like the sabertooth cats and wild dogs (or other scavengers like the hyenas, jackals, and vultures) to surrender the prey carcass (Espigares et al., 2013, 2023). These cobbles could also be used later as percussion tools for fracturing bones and accessing their medullary cavities, as suggested by the finding of percussion marks in half of these manuports (Barsky et al., 2015, 2016, 2022).

The third possibility, i.e. that the hominins had primary access to intact carcasses of animals that died through natural causes (e.g., disease and starvation) or secondary access to the prey leftovers abandoned by primary predators, seems the most reasonable given the anatomy of early *Homo* as well as their apparently limited technological skills (Espigares et al., 2019; Palmqvist et al., 2023a). Apart from vultures, the giant hyena *P. brevirostris* and the jackal-sized dog *C. mosbachensis* would indeed be worthy competitors of the FN3 hominins in the access to carrion (Iannucci et al., 2021; Palmqvist et al., 2011, 2023b). Modern hyenas and jackals often rely upon visual clues such as circling vultures to identify scavengeable resources, and then run long distances to secure the carcass (Bramble and Liberman, 2004). Compared with these terrestrial carnivores, which patterns of activity are more twilight and nocturnal, the hominins were likely predominantly diurnal. This means that the information provided by the aerial scavengers was probably more helpful for the early members of *Homo* than for other terrestrial scavengers. Given that hominins and vultures occupied the same habitats and scavenged the same medium-to-large, large and very large mammals, they likely competed for access to carcasses alongside other terrestrial scavengers like hyenas and jackals (Morelli et al., 2015). Vultures are such efficient scavengers that in some areas of Africa they consume more meat than all other carnivores combined (Ogada et al., 2012), which explains their high diversity. For this reason, it has been suggested that vultures used as beacons for meat were particularly important to the hominins that dispersed out of Africa, facilitating their occupation of new landscapes when they arrived in Europe (see review in Morelli et al., 2015).

According to Liebenberg (2006), endurance or persistence running (i.e., the ability to run many kilometers at relatively low speed over extended time periods using aerobic metabolism) could have been an adaptation of hominins for tracking down and chasing to exhaustion small-to-medium sized ungulates. The reason is that although humans are comparatively poor sprinters, they perform well at running long distances due to several anatomical and physiological adaptations. These include (i) a long tibia, which results in a long stride length combined with the presence of long spring-like tendons connected to short muscle fascicles, which economically generate substantial force; (ii) a long plantar arch and enlarged articular surface areas in most of the joints of the lower body, which dissipate the high impact loads generated in running; (iii) derived features that enhance trunk stabilization, such as an expanded area on the sacrum for attachment of enlarged gluteus muscles; and (iv) thermoregulatory adaptations for heat dissipation that help to maintain stable body temperature, including a multiplication of eccrine sweat glands for evapotranspiration, reduced body hair, mouth breathing, and an elaborated cranial venous circulation for brain cooling (see reviews in Bramble and Liberman, 2004; Liebenberg, 2006; Ruxton & Wilkinson, 2012). Endurance running evolved early in the genus *Homo,* as shown by the modern human-like body proportions and lower limb morphology of the Dmanisi hominins, which are indicative of the ability for long-distance traveling (Lordkipanidze et al., 2007).

The human adaptations discussed above for persistence hunting of small-to-medium sized prey are equally useful for scavenging carcasses of large and very large animals in open habitats during the day, particularly in the dry season, when other terrestrial scavengers like hyenas and jackals avoid running long distances due to thermoregulatory constraints (Bramble and Liberman, 2004; Liebenberg, 2006; Lieberman et al., 2007; Ruxton & Wilkinson, 2012). For this reason, endurance running may have been the key to hominin success in the access to carcasses of large-sized ungulates at FN3 before eventually surrendering them on the arrival of potentially dangerous hyenas or other terrestrial scavengers (Palmqvist et al., 2023a). This scenario is suggested by the finding of a partial skeleton of elephant *M. meridionalis* in the UAL (Fig. 9A), which is partially surrounded by flakes and hyena coprolites (Espigares et al., 2013). Although Yravedra et al. (2021) argued that no tooth marks or anthropogenic marks were observed on the elephantid bones, thus not conclusively proving the interaction of humans or carnivores with the proboscidean carcass (however, for a new interpretation see Yravedra et al., 2024), the spatial association of lithic tools and coprolites with the elephant carcass did not result from independent episodes that coalesced into a palimpsest (Palmqvist et al., 2023a): > 95% of the bones unearthed from FN3 preserve intact their cortical surface, showing weathering stage 0 (Yravedra et al., 2021), which evidences a very short time of exposure before burial, less than one year according to the studies of weathering rates by Behrensmeyer (1978) in Amboseli National Park, Kenya. According to Espigares et al. (2013), this tentatively suggests that the hominids were the first to scavenge the elephant carcass, dismembering and transporting its limbs for later consumption in a safer place, and that the hyenas arrived later and consumed the rest of the carcass, defecating in its surroundings.

All these arguments apply to the bone assemblage accumulated in the UAL of FN3. However, the situation depicted at the LAL was quite different. For this reason, it is worth considering the insights on the role played by hominins and hyenas provided by Palmqvist et al. (2023a), who studied the patterns of bone survival in FN3 and compared them with those detected in the hyena den of VM (Arribas & Palmqvist, 1998). Specifically, Palmqvist et al. (2023a) showed that in both sites there is: (i) a direct relationship between the abundance of skeletal remains of large mammals and their estimated mineral densities; and (ii) an inverse relationship between the survival of major limb bone epiphyses and their estimated marrow yields. However, FN3 shows considerable scatter around both regression lines, which renders these relationships statistically less significant than in VM. According to Palmqvist et al. (2023a), these results suggest that exploitation by the hominins of bone marrow after hammerstone breakage was a usual activity during carcass processing at FN3. As a result, few bones retained their marrow contents after the exploitation of marrow by hominins, which made them less attractive for hyenas. This explains the lower frequency of tooth-marked bones in FN3 compared to VM, where the bone-cracking agency was the hyena *P. brevirostris* (the frequency of tooth-marked bones in VM3, the main excavation quarry of the VM site, is 29.3%; Palmqvist et al., 2022b). The lower selectivity in bone fracturing evidenced at FN3 probably results from the fact that hominins fractured the bones assisted by their limestone manuports. This suggests that the mineral density of the skeletal elements was not as much of a problem for breaking them in the case of hominins as it was in the case of hyenas, which performed this task using their robust jaws and enlarged premolar teeth (Arribas & Palmqvist, 1998; Palmqvist et al., 2011, 2022b). This forced the hyenas to be more selective than the hominins when choosing which skeletal elements to fracture, in order to avoid breaking their teeth or dislocating their jaws when fracturing the densest bones (Palmqvist et al., 2023a).

Palmqvist et al. (2023a) also calculated an index of skeletal completeness that allows estimating ravaging intensity in a skeletal assemblage, the ratio of axial bones to appendicular bones. The value of this ratio in FN3 (0.44) is higher than in VM (0.13), which indicates that the bone assemblage of VM was comparatively more ravaged due to selective transport of the skeletal remains by the hyenas. According to Palmqvist et al. (2023a), the living hyenas do not cooperate in the transportation of large portions of a carcass, which limits the individuals in what they can move and forces them to be more selective. The analysis of skeletal representation for ungulate taxa in VM showed that hyenas selectively transported herbivore carcasses and body parts to their maternity den as a function of the mass of the ungulates scavenged (Palmqvist & Arribas, 2001; Palmqvist et al., 2011): small-to-medium sized ungulates were transported as whole carcasses to the denning area while large and very large-sized species were dismembered and the hyenas preferentially transported the limbs that provided higher marrow yields. This resulted in a low ratio of axial elements to limb bones at VM. In contrast, the higher value of this ratio at FN3 suggests that the carcasses of the ungulates scavenged were less biased by selective transport, which points to cooperative transport of these ungulate carcasses by the hominins (Palmqvist et al., 2023a).

5 Conclusions

The two archaeological levels of the Fuente Nueva-3 (FN3) site, the lower archaeological level (LAL) and the upper archaeological level (UAL), preserve evidence of consumption of ungulate carcasses by both the hominins and hyenas (Espigares et al. 2013, 2019, 2023; Palmqvist et al., 2023a; Yravedra et al., 2021). However, evidence of hominin activity concentrates in the LAL, as evidenced by the abundance of both Oldowan tools and manuports, while most hyena coprolites are found in the UAL, which suggests that the FN3 area was frequently occupied by hyenas during the period of time in which the sediments of layer 5 accumulated. This layer, whose lithology agrees with the expectations from a quicksand, preserves abundant remains of megafauna, particularly young elephants, which suggests the frequent entrapment of large-sized animals in the sediments of layer 5. Given that the resources of these carcasses would remain accessible to the scavengers for longer, the giant hyenas could have made greater use of them, which explains the concentration of coprolites in the UAL of the FN3 site.

Funding Funding for open access publishing: Universidad de Málaga/CBUA.

Declarations

Conflict of interest On behalf of all authors, the corresponding author states that there is no conflict of interest.

Research involving human participants and/or animals This research involved no human participants and/or animals.

Informed consent All authors participated in this research, contributed to elaborating the manuscript contents and agreed in submitting it for publication in Journal of Iberian Geology.

References

Alfaro, P., Gibert, L., Moretti, M., García-Tortosa, F. J., Sanz de Galdeano, C., Galindo-Zaldívar, J., & López-Garrido, A. C. (2010). The significance of giant seismites in the Plio-Pleistocene Baza palaeo-lake (S Spain). *Terra Nova, 22*(3), 172–179. https://doi.org/10.1111/j.1365-3121.2010.00930.x

Alfaro, P., Moretti, M., & Soria, J. M. (1997). Soft-sediment deformation structures induced by earthquakes (seismites) in the Pliocene lacustrine deposits (Guadix-Baza basin, Central Betic Cordillera). *Eclogae Geologicae Helvetiae, 90*, 531–540. https://doi.org/10.5169/seals-168193

Altamura, F., Bennett, M. R., D'Août, K., Gaudzinski-Windheuser, S., Melis, R. T., Reynolds, S. C., & Mussi, M. (2018). Archaeology and ichnology at Gombore II-2, Melka Kunture, Ethiopia: everyday life of a mixed-age hominin group 700,000 years ago. *Scientific Reports, 8*, 2815. https://doi.org/10.1038/s41598-018-21158-7

Altamura, F., Lehmann, J., Rodríguez-Álvarez, B., Urban, B., van Kolfschoten, T., Verheijen, I., Conard, N. J., & Serangeli, J. (2023). Fossil footprints at the late Lower Paleolithic site of Schöningen (Germany): a new line of research to reconstruct animal and hominin paleoecology. *Quaternary Science Reviews, 310*, 108094. https://doi.org/10.1016/j.quascirev.2023.108094

Altamura, F., Melis, R. T., & Mussi, M. (2017). A Middle Pleistocene hippo tracksite at Gombore II-2 (Melka Kunture, Upper Awash, Ethiopia). *Palaeogeography Palaeoclimatology Palaeoecology, 470*, 122–131. https://doi.org/10.1016/j.palaeo.2017.01.022

Álvarez, C., Parés, J. M., Granger, D., Duval, M., Sala, R., & Toro, I. (2015). New magnetostratigraphic and numerical age of the Fuente Nueva-3 site (Guadix-Baza basin, Spain). *Quaternary International, 389*, 224–234. https://doi.org/10.1016/j.quaint.2015.04.044

Anadón, P., Julià Brugués, R., & Oms, O. (2003). Estratigrafía y estudio sedimentológico preliminar de diversos afloramientos en Barranco León y Fuente Nueva (Orce, Granada). Memoria Científica campañas 1999–2002. In: Toro, I., Agustí, J., Martínez Navarro, B. (Eds.), El Pleistoceno inferior de Barranco León y Fuente Nueva 3, Orce (Granada). Junta de Andalucía. Consejería de Cultura, Arqueología Monografías, Sevilla, 47–72.

Anadón, P., Oms, O., Riera, V., & Julià, R. (2015). The geochemistry of biogenic carbonates as a paleoenvironmental tool for the Lower Pleistocene Barranco León sequence (BL-5D, Baza Basin, Spain). *Quaternary International, 389*, 70–83. https://doi.org/10.1016/j.quaint.2014.09.062

Anadón, P., Utrilla, R., & Julià, R. (1994). Palaeoenvironmental reconstruction of a Pleistocene lacustrine sequence from faunal assemblages and ostracode shell geochemistry. Baza Basin, SE Spain. *Palaeogeography Palaeoclimatology Palaeoecology, 111*, 191–205. https://doi.org/10.1016/0031-0182(94)90062-0

Arribas, A., & Palmqvist, P. (1998). Taphonomy and paleoecology of an assemblage of large mammals: hyaenid activity in the lower Pleistocene site at Venta Micena (Orce, Guadix-Baza Basin, Granada, Spain). *Geobios, 31*, 3–47. https://doi.org/10.1016/S0016-6995(98)80056-9

Barsky, D., Sala, R., Menéndez, L., & Toro-Moyano, I. (2015). Use and re-use: Re-knapped flakes from the Mode 1 site of Fuente Nueva 3 (Orce, Andalucía, Spain). *Quaternary International, 361*, 21–33. https://doi.org/10.1016/j.quaint.2014.01.048

Barsky, D., Titton, S., Sala-Ramos, R., Bargalló, A., Grégoire, S., Saos, T., Serrano-Ramos, A., Oms, O., Solano-García, J. A., Toro-Moyano, I., & Jiménez-Arenas, J. M. (2022). The significance of subtlety: Contrasting lithic raw materials procurement and use patterns at the Oldowan sites of Barranco León and Fuente Nueva 3 (Orce, Andalusia, Spain). *Frontiers in Earth Science, 10*, 893776. https://doi.org/10.3389/feart.2022.893776

Barsky, D., Vergès, J. M., Sala, R., Menéndez, L., & Toro-Moyano, I. (2016). Limestone percussion tools from the late Early Pleistocene sites of Barranco León and Fuente Nueva 3 (Orce, Spain). *Philosophical Transactions of the Royal Society B, 370*, 20140352. https://doi.org/10.1098/rstb.2014.0352

Bartolini-Lucenti, S., Madurell-Malapeira, J., Martínez-Navarro, B., Cirilli, O., Pandolfi, L., Rook, L., Bushkhianidze, M., & Lordkipanidze, D. (2022). A comparative study of the Early Pleistocene carnivore guild from Dmanisi (Georgia). *Journal of Human Evolution, 162*, 103108. https://doi.org/10.1016/j.jhevol.2021.103108

Bartolini-Lucenti, S., Madurell-Malapeira, J., Martínez-Navarro, B., Palmqvist, P., Lordkipanidze, D., & Rook, L. (2021). The early hunting dog from Dmanisi with comments on the social behaviour in Canidae and hominins. *Scientific Reports, 11*, 13501. https://doi.org/10.1038/s41598-021-92818-4

Behrensmeyer, A. K. (1978). Taphonomic and ecologic information from bone weathering. *Paleobiology, 4*, 150–162. https://doi.org/10.1017/S0094837300005820

Behrensmeyer, A. K., & Laporte, L. F. (1981). Footprints of a Pleistocene hominid in northern Kenya. *Nature, 289*, 167–169. https://doi.org/10.1038/289167a0

Bennett, M. R., Morse, S. A., & Falkingham, P. L. (2014). Tracks made by swimming Hippopotami: an example from Koobi Fora (Turkana Basin, Kenya). *Palaeogeography Palaeoclimatology Palaeoecology, 409*, 9–23. https://doi.org/10.1016/j.palaeo.2014.04.021

Blott, S., & Pye, K. (2001). Gradistat: a grain size distribution and statistics package for the analysis of unconsolidated sediments. *Earth Surface Processes and Landforms, 26*, 1237–1248. https://doi.org/10.1002/esp.261

Blumenschine, R. J., & Pobiner, B. L. (2007). Zooarchaeology and the ecology of Oldowan hominin carnivory. In P. Ungar (Ed.), Evolution of the human diet: the known, the unknown, and the unknowable (1st ed., pp. 167–190). Oxford University Press, Oxford.

Boisserie, J. R. (2005). The phylogeny and taxonomy of Hippopotamidae (Mammalia, Artiodactyla), a review based on morphology and cladistic analysis. *Zoological Journal of the Linnean Society, 143*(1), 1–26. https://doi.org/10.1111/j.1096-3642.2004.00138.x

Bout-Roumazeilles, V., Combourieu Nebout, N., Peyron, O., Cortijo, E., Landais, A., & Masson-Delmotte, V. (2007). Connection between South Mediterranean climate and North African atmospheric circulation during the last 50,000 yrBP North Atlantic cold events. *Quaternary Science Reviews, 26*, 3197–3215. https://doi.org/10.1016/j.quascirev.2007.07.015

Braga, J. C., Martín, J. M., & Quesada, C. (2003). Patterns and average rates of late Neogene-Recent uplift of the Betic Cordillera, SE Spain. *Geomorphology, 50*, 3–26. https://doi.org/10.1016/S0169-555X(02)00205-2

Bramble, D., & Lieberman, D. (2004). Endurance running and the evolution of *Homo*. *Nature, 432*, 345–352. https://doi.org/10.1038/nature03052

Carbonell, E., Bermúdez de Castro, J. M., Parés, J. M., Pérez-González, A., Cuenca-Bescós, G., Ollé, A., Mosquera, M., Huguet, R., van der Made, J., Rosas, A., Sala, R., Valverdú, J., García, N., Granger, D. E., Martinón-Torres, M., Rodríguez, X. P., Stock, G. M., Vergès, J. M., Allué, E., … Arsuaga, J. L. (2008). The first hominin of Europe. *Nature, 452*, 465–470. https://doi.org/10.1038/nature06815

Cherin, M., Alba, D. M., Crotti, M., Menconero, S., Moullé, P.-E., Sorbelli, L., & Madurell-Malapeira, J. (2020). The post-Jaramillo persistence of *Sus strozzii* (Suidae, Mammalia) in Europe: New evidence from the Vallparadís Section (NE Iberian Peninsula) and other coeval sites. *Quaternary Science Reviews, 233*, 106234. https://doi.org/10.1016/j.quascirev.2020.106234

Cherin, M., Sorbelli, L., Crotti, M., Iurino, D. A., Sardella, R., & Souron, A. (2018). New material of *Sus strozzii* (Suidae, Mammalia) from the Early Pleistocene of Italy and a phylogenetic analysis of suines. *Quaternary Science Reviews, 194*, 94–115. https://doi.org/10.1016/j.quascirev.2018.06.029

Coil, R., Tappen, M., Ferring, R., Bukhsianidze, M., Nioradze, M., & Lordkipanidze, D. (2020). Spatial patterning of the archaeological and paleontological assemblage at Dmanisi, Georgia: An analysis of site formation and carnivore-hominin interaction in Block 2. *Journal of Human Evolution, 143*, 102773. https://doi.org/10.1016/j.jhevol.2020.102773

Courtenay, L. A., Yravedra, J., Herranz-Rodrigo, D., Rodríguez-Alba, J. J., Serrano-Ramos, A., Estaca-Gómez, V., González-Aguilera, D., Solano, J. A., & Jiménez-Arenas, J. M. (2023). Deciphering carnivoran competition for animal resources at the 1.46 Ma early Pleistocene site of Barranco León (Orce, Granada, Spain). *Quaternary Science Reviews, 300*, 107912. https://doi.org/10.1016/j.quascirev.2022.107912

Craig, R. F. (1997). *Soil mechanics*. Chapman & Hall.

Deino, A. L. (2010). ^{40}Ar/^{39}Ar dating of Laetoli, Tanzania. In T. Harrison (Ed.), Paleontology and geology of Laetoli: Human evolution in context. *Vertebrate Paleobiology and Paleoanthropology Series* (1st. ed., pp. 77−97). Springer, Dordrecht. https://doi.org/10.1007/978-90-481-9956-34

Duval, M., Falguères, C., Bahain, J. J., Grün, R., Shao, Q., Aubert, M., Dolo, J. M., Agustí, J., Martínez-Navarro, B., Palmqvist, P., & Toro-Moyano, I. (2012). On the limits of using combined U-series/ESR method to date fossil teeth from two Early Pleistocene archaeological sites of the Orce area (Guadix-Baza basin, Spain). *Quaternary Research, 77*(3), 481–482. https://doi.org/10.1016/j.yqres.2012.01.003

Elbaz, K., Shen, J. S., Arulrajah, A., & Horpibulsuk, S. (2016). Geohazards induced by anthropic activities of geoconstruction: A review of recent failure cases. *Arabian Journal of Geosciences, 9*, 708. https://doi.org/10.1007/s12517-016-2740-z

Escudero, M., Stein, A. F., Draxler, R. R., Querol, X., Alastuey, A., Castillo, S., & Avila, A. (2011). Source apportionment for African dust outbreaks over the Western Mediterranean using the HYSPLIT model. *Atmospheric Research, 99*(3–4), 518–527. https://doi.org/10.1016/j.atmosres.2010.12.002

Espigares, M. P. (2010). Análisis y modelización del contexto sedimentario y los atributos tafonómicos de los yacimientos pleistocénicos del borde nororiental de la cuenca de Guadix-Baza. PhD Thesis Dissertation. University of Granada, Spain, p 533. https://digibug.ugr.es/handle/10481/4949?locale-attribute=en

Espigares, M. P., Martínez-Navarro, B., Palmqvist, P., Ros-Montoya, S., Toro, I., Agustí, J., & Sala, R. (2013). *Homo* vs. *Pachycrocuta:* Earliest evidence of competition for an elephant carcass between scavengers at Fuente Nueva-3 (Orce, Spain). *Quaternary International, 295*, 113–125. https://doi.org/10.1016/j.quaint.2012.09.032

Espigares, M. P., Palmqvist, P., Guerra-Merchán, A., Ros-Montoya, S., García-Aguilar, J. M., Rodríguez-Gómez, G., Serrano, F. J., & Martínez-Navarro, B. (2019). The earliest cut marks of Europe: A discussion on hominin subsistence patterns in the Orce sites (Baza basin, SE Spain). *Scientific Reports, 9*, 15408. https://doi.org/10.1038/s41598-019-51957-5

Espigares, M. P., Palmqvist, P., Rodríguez-Ruiz, M. D., Ros-Montoya, S., Pérez-Ramos, A., Rodríguez-Gómez, G., Guerra-Merchán, A., García-Aguilar, J. M., Granados, A., Campaña, I., & Martínez-Navarro, B. (2023). Sharing food with hyenas: A latrine of *Pachycrocuta brevirostris* in the Early Pleistocene assemblage of Fuente Nueva-3 (Orce, Baza Basin, SE Spain). *Archaeological and Anthropological Sciences, 15*, 81. https://doi.org/10.1007/s12520-023-01784-7

Fall, A., Weber, B., Pakpour, M., Lenoir, N., Shahidzadeh, N., Fiscina, J., Wagner, C., & Bonn, D. (2014). Sliding friction on wet and dry sand. *Physical Review Letters, 112*(17), 175502. https://doi.org/10.1103/PhysRevLett.112.175502

Fuhrmann, R. (2012). Atlas quartärer und rezenter Ostrakoden Mitteldeutschlands (pp. 1–320). Altenburg: Naturkundliches Museum Mauritianum.

Gao, G., Yao, S., Cui, Y., Chen, Q., Zhang, X., & Wang, K. (2018). Zoning of confined aquifers inrush and quicksand in Shanghai region. *Natural Hazards, 91*, 1341–1363. https://doi.org/10.1007/s11069-018-3189-z

García-Aguilar, J. M., Guerra-Merchán, A., Serrano, F., Flores-Moya, A., Delgado-Huertas, A., Espigares, M. P., Ros-Montoya, S., Martínez-Navarro, B., & Palmqvist, P. (2015). A reassessment of the evidence for hydrothermal activity in the Neogene-Quaternary lacustrine environments of the Baza basin (Betic Cordillera, SE Spain) and its paleoecological implications. *Quaternary Science Reviews, 112*, 226–235. https://doi.org/10.1016/j.quascirev.2015.02.001

García-Aguilar, J. M., Guerra-Merchán, A., Serrano, F., Palmqvist, P., Flores-Moya, A., & Martínez-Navarro, B. (2014). Hydrothermal activity and its paleoecological implications in the latest Miocene to Middle Pleistocene lacustrine environments of the Baza Basin (Betic Cordillera, SE Spain). *Quaternary Science Reviews, 96*, 204–221. https://doi.org/10.1016/j.quascirev.2013.07.009

García-Aguilar, J. M., & Palmqvist, P. (2011). A model of lacustrine sedimentation for the Lower Pleistocene deposits of Guadix-Baza basin (southeast Spain). *Quaternary International, 243*(1), 3–15. https://doi.org/10.1016/j.quaint.2011.02.008

García-Tortosa, F. J., Alfaro, P., Sanz de Galdeano, C., & Galindo-Zaldívar, J. (2011). Glacis geometry as a geomorphic marker of recent tectonics: The Guadix-Baza basin (South Spain). *Geomorphology, 125*, 517–529. https://doi.org/10.1016/j.geomorph.2010.10.021

Gibert, L., Sanz de Galdeano, C., Alfaro, P., Scott, G., & López Garrido, A. C. (2005). Seismic-induced slump in Early Pleistocene deltaic deposits of the Baza Basin (SE Spain). *Sedimentary Geology, 179*(3–4), 279–294. https://doi.org/10.1016/j.sedgeo.2005.06.003

Granados, A., Oms, O., Anadón, P., Ibáñez-Insa, J., Kaakinen, A., & Jiménez-Arenas, J. M. (2021). Geochemical and sedimentary constraints on the formation of the Venta Micena Early Pleistocene site (Guadix-Baza basin, Spain). *Scientific Reports, 11*(1), 22437. https://doi.org/10.1038/s41598-021-01711-7

Günster, N., Eck, P., Skowronek, A., & Zöller, L. (2001). Late Pleistocene loess and their paleosols in the Granada Basin, Southern Spain. *Quaternary International, 76–77*, 241–245. https://doi.org/10.1016/S1040-6182(00)00106-3

Harington, C. R., Grant, D. R., & Mott, R. J. (1993). The Hillsborough, New Brunswick, mastodon and comments on other Pleistocene mastodon fossils from Nova Scotia. *Canadian Journal of Earth Sciences, 30*, 1242–2125. https://doi.org/10.1139/e93-106

Hungerbühler, A. (1998). Taphonomy of the prosauropod dinosaur *Sellosaurus,* and its implications for carnivore faunas and feeding habits in the Late Triassic. *Palaeogeography Palaeoclimatology Palaeoecology, 143*(1–3), 1–29. https://doi.org/10.1016/S0031-0182(98)00074-1

Hüsing, S. K., Oms, O., Agustí, J., Garcés, M., Kouwenhoven, T. J., Krijgsman, W., & Zachariasse, W. J. (2010). On the late Miocene closure of the Mediterranean-Atlantic gateway through the Guadix basin (Southern Spain). *Palaeogeography Palaeoclimatology Palaeoecology, 291*(3–4), 167–179. https://doi.org/10.1016/j.palaeo.2010.02.005

Iannucci, A. (2024). The occurrence of suids in the post-Olduvai to pre-Jaramillo Pleistocene of Europe and implications for Late Villafranchian biochronology and faunal dynamics. *Quaternary, 7*, 11. https://doi.org/10.3390/quat7010011

Iannucci, A., Mecozzi, B., Sardella, R., & Iurino, D. A. (2021). The extinction of the giant hyena *Pachycrocuta brevirostris* and a reappraisal of the Epivillafranchian and Galerian Hyaenidae in Europe: Faunal turnover during the Early-Middle Pleistocene Transition. *Quaternary Science Reviews, 272*, 107240. https://doi.org/10.1016/j.quascirev.2021.10724

Jachmann, H. (2001). Estimating abundance of African wildlife: An aid to adaptive management. *Kluwer Academic Publishers*. https://doi.org/10.1007/978-1-4615-1381-0

Kadau, D., Herrmann, H. J., Andrade, J. S., Araújo, A. D., Bezerra, L. J. C., & Maia, L. P. (2009). Living quicksand. *Granular Matter, 11*, 67–71. https://doi.org/10.1007/s10035-008-0117-z

Khaldoun, A., Eiser, E., Wegdam, G., & Bonn, D. (2005). Liquefaction of quicksand under stress. *Nature, 437*, 635. https://doi.org/10.1038/437635a

Khaldoun, A., Eiser, E., Wegdam, G., & Bonn, D. (2006). Quicksand! *Europhysics News, 37*, 18–19. https://doi.org/10.1051/epn:2006404

Lawley, D. N. (1938). A generalization of Fisher's z-test. *Biometrika, 30*(1–2), 180–187. https://doi.org/10.1093/biomet/30.1-2.180

Lawrence, C. R., & Neff, J. C. (2009). The contemporary physical and chemical flux of aeolian dust: A synthesis of direct measurements of dust deposition. *Chemical Geology, 267*(1–2), 46–63. https://doi.org/10.1016/j.chemgeo.2009.02.005

Leakey, M., & Hay, R. (1979). Pliocene footprints in the Laetolil Beds at Laetoli, northern Tanzania. *Nature, 278*, 317–323. https://doi.org/10.1038/278317a0

Liebenberg, L. (2006). Persistence hunting by modern hunter-gatherers. *Current Anthropology, 47*, 1017–1026. https://doi.org/10.1086/508695

Lieberman, D. E., Bramble, D. M., Raichlen, D. A., & Shea, J. J. (2007). The evolution of endurance running and the tyranny of ethnography: A reply to Pickering and Bunn. *Journal of Human Evolution, 53*(4), 439–442. https://doi.org/10.1016/j.jhevol.2007.07.002

Liefferink, R. W., Aliasgari, M., Maleki-Jirsaraei, N., Rouhani, S., & Bonn, D. (2020). Sliding on wet sand. *Granular Matter, 22*, 1–6. https://doi.org/10.1007/s10035-020-01022-0

Lordkipanidze, D. O. (2015). The traces of the first humans in Eurasia. In N. Sanz (Ed.), Human origin sites and the World Heritage Convention in Eurasia, World Heritage Papers 41, vol. I (1st ed., pp. 153–162). Unesco.

Lordkipanidze, D. O., Jashashvili, T., Vekua, A., Ponce de León, M. S., Zollikofer, C. P. E., Rightmire, G. P., Pontzer, H., Ferring, R., Oms, O., Tappen, M., Bukhsianidze, M., Agusti, J., Kahlke, R., Kiladze, G., Martinez-Navarro, B., Mouskhelishvili, A., Nioradze, M., & Rook, L. (2007). Postcranial evidence from early *Homo* from Dmanisi, Georgia. *Nature, 449*, 305–310. https://doi.org/10.1038/nature06134

Lundegard, P. D. (1992). Sandstone porosity loss; a "big picture" view of the importance of compaction. *Journal of Sedimentary Petrology, 62*(2), 250–260. https://doi.org/10.1306/D42678D4-2B26-11D7-8648000102C1865D

Madurell-Malapeira, J., Minwer-Barakat, R., Alba, D. M., Garcés, M., Gómez, M., Aurell-Garrido, J., Ros-Montoya, S., Moyà-Solà, S., & Berástegui, X. (2010). The Vallparadís section (Terrassa, Iberian Peninsula) and the latest Villafranchian faunas of Europe. *Quaternary Science Reviews, 29*(27–28), 3972–3982. https://doi.org/10.1016/j.quascirev.2010.09.020

Madurell-Malapeira, J., Ros-Montoya, S., Espigares, M. P., Alba, D. M., & Aurell-Garrido, J. (2014). Villafranchian large mammals from the Iberian Peninsula: Paleobiogeography, paleoecology and dispersal events. *Journal of Iberian Geology, 40*, 167–178. https://doi.org/10.5209/rev_JIGE.2014.v40.n1.44093

Maldonado-Garrido, E., Piñero, P., & Agustí, J. (2017). A catalogue of the vertebrate fossil record from the Guadix-Baza Basin (SE Spain). *Spanish Journal of Paleontology, 32*(1), 207–236. https://doi.org/10.7203/sjp.32.1.17040

Marfil, R., & De la Peña, J. A. (1989). Diagénesis: Rocas siliciclásticas y rocas carbonáticas. In A. Arche (Ed.), Sedimentología, Vol. II (1st ed., pp., 343–427). CSIC, Madrid.

Martínez Navarro, B., 1991. Revisión Sistemáica y estudio cuantitativo de la fauna de macromamiferos del yacimiento de Venta Micena

(Orce, Granada). Ph.D. dissertation. Universitat Autónoma de Barcelona, Bellaterra, p. 334.

Martínez-Navarro, B., Palmqvist, P., Madurell-Malapeira, J., Ros-Montoya, S., Espigares, M.P., Torregrosa, V., & Pérez-Claros, J.A. (2010). La fauna de grandes mamíferos de Fuente Nueva 3 y Barranco León 5. Estado de la cuestión. In I. Toro, B. Martínez-Navarro, J. Agustí (Eds.), Ocupaciones humanas en el Pleistoceno inferior y medio de la cuenca de Guadix-Baza, Memoria Científica. Junta de Andalucía. Consejería de Cultura. Arqueología Monografías, pp. 197–236.

Martínez-Navarro, B., Belmaker, M., & Bar-Yosef, O. (2009). The large carnivores from 'Ubeidiya (Early Pleistocene, Israel): Biochronological and biogeographical implications. *Journal of Human Evolution, 56*(5), 514–524. https://doi.org/10.1016/j.jhevol.2009.02.004

Martínez-Navarro, B., Espigares, M. P., Pastó, I., Ros-Montoya, S., & Palmqvist, P. (2014). Early Homo fossil records of Europe. In: C. Smith (Ed.) Encyclopedia of Global Archaeology (1st ed., pp. 2561–2570). Springer.

Martínez-Navarro, B., Ros-Montoya, S., Espigares, M. P., Madurell-Malapeira, J., & Palmqvist, P. (2018). Los mamíferos del Plioceno y Pleistoceno de la Península Ibérica. Revista PH 94, 206–249. https://doi.org/10.33349/2018.0

Martínez-Navarro, B., Madurell-Malapeira, J., Ros-Montoya, S., Espigares, M. P., Medin, T., Hortolà, P., & Palmqvist, P. (2015). The Epivillafranchian and the arrival of pigs into Europe. *Quaternary International, 389*, 131–138. https://doi.org/10.1016/j.quaint.2015.09.039

Martínez-Navarro, B., Turq, A., Agustí, J., & Oms, O. (1997). Fuente Nueva-3 (Orce, Granada, Spain) and the first human occupation of Europe. *Journal of Human Evolution, 33*(5), 611–620. https://doi.org/10.1006/jhev.1997.0158

Masao, F. T., Ichumbaki, E. B., Cherin, M., Barili, A., Boschian, G., Iurino, D. A., Menconero, S., Moggi-Cecchi, J., & Manzi, G. (2016). New footprints from Laetoli (Tanzania) provide evidence for marked body size variation in early hominins. *eLife, 5*, e19568. https://doi.org/10.7554/eLife.19568

Matthes, G. H. (1953). Quicksand. *Scientific American,* 188(6), 97–104. https://www.jstor.org/stable/24944256

Medin, T., Martínez-Navarro, B., Madurell-Malapeira, J., Figueirido, B., Kopaliani, G., Rivals, F., Kiladze, G., Palmqvist, P., & Lordkipanidze, D. (2019). The bears from Dmanisi and the first dispersal of early Homo out of Africa. *Scientific Reports, 9*, 17752. https://doi.org/10.1038/s41598-019-54138-6

Mendoza, M., Janis, C. M., & Palmqvist, P. (2006). Estimating the body mass of extinct ungulates: A study on the use of multiple regression. *Journal of Zoology, 270*, 90–101. https://doi.org/10.1111/j.1469-7998.2006.00094.x

Morelli, F., Kubicka, A. M., Tryjanowski, P., & Nelson, E. (2015). The vulture in the sky and the hominin on the land: Three million years of human–vulture interaction. *Anthrozoös, 28*(3), 449–468. https://doi.org/10.1080/08927936.2015.1052279

Moullé, P. E., Lacombat, F., & Echassoux, A. (2006). Contribution of the large mammals of Vallonnet cave (Roquebrune-Cap-Martin, Alpes-Maritimes, France) to the knowledge of biochronological frame of the second half of the Lower Pleistocene in Europe. *L'anthropologie, 110*(5), 837–849. https://doi.org/10.1016/j.anthro.2006.10.006

Moullé, P. E., Lacombat, F., & Echassoux, A. (2006). Apport des grands mammifères de la grotte du Vallonnet (Roquebrune-Cap-Martin, Alpes-Maritimes, France) à la connaissance du cadre biochronologique de la seconde moitié du Pléistocène inférieur d'Europe. *L'anthropologie, 110*, 837–849. https://doi.org/10.1016/j.anthro.2006.10.006

Neto de Carvalho, C., Belaústegui, Z., Toscano, A., Muñiz, F., Belo, J., Galán, J. M., Gómez, P., Cáceres, L. M., Rodríguez-Vidal, J., Proença Cunha, P., Cachao, M., Ruiz, F., Ramirez-Cruzado, S., Giles-Guzmán, F., Finlayson, G., Finlayson, S., & Finlayson, C. (2021). First tracks of newborn straight-tusked elephants (*Palaeoloxodon antiquus*). *Scientific Reports, 11*, 17311. https://doi.org/10.1038/s41598-021-96754-1

Nguyen, D. L., Ohtsuka, S., Hoshina, T., & Isobe, K. (2016). Discussion on size effect of footing in ultimate bearing capacity of sandy soil using rigid plastic finite element method. *Soils and Foundations, 56*(1), 93–103. https://doi.org/10.1016/j.sandf.2016.01.007

Nomade, S., Pastre, J.-F., Guillou, H., Faure, M., Guérin, C., Delson, E., Debard, E., Voinchet, P., & Msessager, E. (2014). ^{40}Ar/^{39}Ar constraints on some French landmark Late Pliocene to Early Pleistocene large mammalian paleofaunas: Paleoenvironmental and paleoecological implications. *Quaternary Geochronology, 21*, 2–15. https://doi.org/10.1016/j.quageo.2012.12.006

Ogada, D. L., Keesing, F., & Virani, M. Z. (2012). Dropping dead: Causes and con sequences of vulture population declines worldwide. *Annals of the New York Academy of Sciences, 1249*, 57–71. https://doi.org/10.1111/j.1749-6632.2011.06293.x

Oms, O., Anadón, P., Agustí, J., & Julià, R. (2011). Geology and chronology of the continental Pleistocene archaeological and paleontological sites of the Orce area (Baza basin, Spain). *Quaternary International, 243*(1), 33–43. https://doi.org/10.1016/j.quaint.2011.03.048

Oms, O., Parés, J. M., Martínez-Navarro, B., Agustí, J., Toro, I., Martínez-Fernández, G., & Turq, A. (2000). Early human occupation of Western Europe: Paleomagnetic dates for two Paleolithic sites in Spain. *Proceedings of the National Academy of Sciences USA, 97*, 10666–10670. https://doi.org/10.1073/pnas.1803197

Palmqvist, P., & Arribas, A. (2001). Taphonomic decoding of the paleobiological information locked in a lower Pleistocene assemblage of large mammals. *Paleobiology, 27*(3), 512–530. https://doi.org/10.1666/0094-8373(2001)027%3c0512:TDOTPI%3e2.0.CO;2

Palmqvist, P., Duval, M., Diéguez, A., Ros-Montoya, S., & Espigares, M. P. (2016). On the fallacy of using orthogenetic models of rectilinear change in arvicolid teeth for estimating the age of the first human settlements in Western Europe. *Historical Biology, 28*(6), 734–752. https://doi.org/10.1080/08912963.2015.1025390

Palmqvist, P., Martínez-Navarro, B., & Arribas, A. (1996). Prey selection by terrestrial carnivores in a Lower Pleistocene paleocommunity. *Paleobiology, 22*(4), 514–534. https://doi.org/10.1017/S009483730001650X

Palmqvist, P., Martínez-Navarro, B., Pérez-Claros, J. A., Torregrosa, T., Figueirido, B., Jiménez-Arenas, J. M., Espigares, M. P., Ros-Montoya, S., & De Renzi, M. (2011). The giant hyena *Pachycrocuta brevirostris:* Modelling the bone-cracking behavior of an extinct carnivore. *Quaternary International, 243*, 61–79. https://doi.org/10.1016/j.quaint.2010.12.035

Palmqvist, P., Martínez-Navarro, B., Toro, I., Espigares, M. P., Ros-Montoya, S., Torregrosa, V., & Pérez-Claros, J. A. (2005). Réévaluation de la présence humaine au Pléistocène inférieur dans le Sud de l'Espagne. *L'anthropologie, 109*, 411–450. https://doi.org/10.1016/j.anthro.2005.06.001

Palmqvist, P., Rodríguez-Gómez, G., Bermúdez de Castro, J. M., García-Aguilar, J. M., Espigares, M. P., Figueirido, B., Ros-Montoya, S., Granados, A., Serrano, F. J., Martínez-Navarro, B., & Guerra-Merchán, A. (2022a). Insights on the Early Pleistocene hominin population of the Guadix-Baza Depression (SE Spain) and a review on the ecology of the first peopling of Europe. *Frontiers in Ecology and Evolution, 10*, 881651. https://doi.org/10.3389/fevo.2022.881651

Palmqvist, P., Espigares, M. P., Pérez-Claros, J. A., Figueirido, B., Guerra-Merchán, A., Ros-Montoya, S., Rodríguez-Gómez, G., García-Aguilar, J. M., Granados, A., & Martínez-Navarro, B. (2022b). Déjà vu: A reappraisal of the taphonomy of quarry

VM4 of the Early Pleistocene site of Venta Micena (Baza Basin, SE Spain). *Scientific Reports, 12*, 705. https://doi.org/10.1038/s41598-021-04725-3

Palmqvist, P., Rodríguez-Gómez, G., Figueirido, B., García-Aguilar, J. M., & Pérez-Claros, J. A. (2022c). On the ecological scenario of the first hominin dispersal out of Africa. *L'Anthropologie, 126*, 102998. https://doi.org/10.1016/j.anthro.2022.102998

Palmqvist, P., Rodríguez-Gómez, G., Martínez-Navarro, B., Espigares, M. P., Figueirido, B., Ros-Montoya, S., Guerra-Merchán, A., Granados, A., García-Aguilar, J. M., & Pérez-Claros, J. A. (2023a). Déjà vu: On the use of meat resources by sabretooth cats, hominins, and hyaenas in the Early Pleistocene site of Fuente Nueva 3 (Guadix-Baza Depression, SE Spain). *Archaeological and Anthropological Sciences, 15*, 17. https://doi.org/10.1007/s12520-022-01712-1

Palmqvist, P., Rodríguez-Gómez, G., Martínez-Navarro, B., Ros-Montoya, S., Martín-Serra, A., Granados, A., Guerra-Merchán, A., & Espigares, M. P. (2023b). Hominins and carnivores in the Early Pleistocene site of Barranco León (Orce, Baza Basin, SE Spain): Comment on Courtenay et al. (2023b). *Quaternary Science Reviews,* 310, 108120. https://doi.org/10.1016/j.quascirev.2023.108120.

Pasenko, M. R. (2017). Quantitative and qualitative data of footprints produced by Asian (*Elephas maximus*) and African (*Loxodonta africana*) elephants and with a discussion of significance towards fossilized proboscidean footprints. *Quaternary International, 443*, 221–227. https://doi.org/10.1016/j.quaint.2017.05.030

Patchick, P. F. (1966). Quicksand and Water Wells. *Groundwater, 4*, 32–46. https://doi.org/10.1111/j.1745-6584.1966.tb01597.x

Petrucci, M., Cipullo, A., Martínez-Navarro, B., Rook, L., & Sardella, R. (2013). The Late Villafranchian (Early Pleistocene) carnivores (Carnivora, Mammalia) from Pirro Nord (Italy). *Palaeontographica Abteilung A: Paläozoologie – Stratigraphie,* 298,113–145. https://doi.org/10.1127/pala/298/2013/113

Potts, R. (1991). Why the Oldowan? Plio-Pleistocene toolmaking and the transport of resources. *Journal of Anthropological Research, 47*(2), 153–176. https://doi.org/10.1086/jar.47.2.3630323

Ren, L., & Hutchinson, J. R. (2008). The three-dimensional locomotor dynamics of African (*Loxodonta africana*) and Asian (*Elephas maximus*) elephants reveal a smooth gait transition at moderate speed. *Journal of the Royal Society Interface, 5*, 195–211. https://doi.org/10.1098/rsif.2007.1095

Ren, L., Miller, C. E., Lair, R., & Hutchinson, J. R. (2010). Integration of biomechanical compliance, leverage, and power in elephant limbs. *Proceedings of the National Academy of Sciences, 107*(15), 157078–157082. https://doi.org/10.1073/pnas.0911396107

Rodríguez-Gómez, G., Palmqvist, P., Rodríguez, J., Mateos, A., Martín-González, J. A., Espigares, M. P., Ros-Montoya, S., & Martínez-Navarro, B. (2016a). On the ecological context of the earliest human settlements in Europe: Resource availability and competition intensity in the carnivore guild of Barranco León-D and Fuente Nueva-3 (Orce, Baza Basin, SE Spain). *Quaternary Science Reviews, 134*, 69–83. https://doi.org/10.1016/j.quascirev.2016.05.018

Rodríguez-Gómez, G., Mateos, A., Martín-González, J. A., & Rodríguez, J. (2016b). Measuring intraguild competition from faunal assemblages to compare environmental conditions among paleocommunities. *Quaternary International,* 413(B), 55–68. https://doi.org/10.1016/j.quaint.2015.11.087

Rodríguez-Gómez, G., Martín-González, J. A., Espigares, M. P., Bermúdez de Castro, J. M., Martínez-Navarro, B., Arsuaga, J. L., & Palmqvist, P. (2024). From meat availability to hominin and carnivore biomass: A paleosynecological approach to reconstructing predator-prey biomass ratios in the Pleistocene. *Quaternary Science Reviews, 328*, 108474. https://doi.org/10.1016/j.quascirev.2023.108474

Rodríguez-Gómez, G., Palmqvist, P., Martínez-Navarro, B., Martín-González, J. A., & Bermúdez de Castro, J. M. (2022). Mean body size estimation in large mammals and the computation of biomass in past ecosystems: An application to the Pleistocene sites of Orce and Sierra de Atapuerca (Spain). *Comptes Rendus Palevol, 21*, 207–233. https://doi.org/10.5852/cr-palevol2022v21a10

Rodríguez-Gómez, G., Palmqvist, P., Ros-Montoya, S., Espigares, M. P., & Martínez-Navarro, B. (2017). Resource availability and competition intensity in the carnivore guild of the Early Pleistocene site of Venta Micena (Orce, Baza Basin, SE Spain). *Quaternary Science Reviews, 164*, 154–167. https://doi.org/10.1016/j.quascirev.2017.04.006

Ros-Montoya, S., Bartolini-Lucenti, S., Espigares, M. P., Palmqvist, P., & Martinez-Navarro, B. (2021). First review of the lyncodontini material (Mustelidae, Carnivora, Mammalia) from the lower pleistocene archaeo-palaeontological sites of Orce (Southeastern Spain). *Rivista Italiana di Paleontologia e Stratigrafia, 127*(1), 33–47. https://doi.org/10.13130/2039-4942/15132

Ruxton, G. D., & Wilkinson, D. M. (2012). Endurance running and its relevance to scavenging by early hominins. *Evolution, 67*(3), 861–867. https://doi.org/10.1111/j.1558-5646.2012.01815.x

Shanghai Urban-Rural Construction and Transportation Commission (SUCTC). (2012). Code for investigation of geotechnical engineering (DGJ08–37–2012). Shanghai, China.

Soria, J. M., Fernández, J., & Viseras, C. (1999). Late Miocene stratigraphy and palaeogeographic evolution of the intramontane Guadix Basin (Central Betic Cordillera, Spain): Implications for an Atlantic-Mediterranean connection. *Palaeogeography Palaeoclimatology Palaeoecology, 151*(4), 255–266. https://doi.org/10.1016/S0031-0182(99)00019-X

Sun, Y.-Y. (2016). Experimental and theoretical investigation on the stability of deep excavations against confined aquifers in Shanghai, China. *KSCE Journal of Civil Engineering, 20*(7), 2746–2754. https://doi.org/10.1007/s12205-016-0488-3

Titton, S., Barsky, D., Bargalló, A., Vergès, J. M., Guardiola, M., García-Solano, J., Jiménez-Arenas, J. M., Toro-Moyano, I., & Sala-Ramos, R. (2018). Active percussion tools from the Oldowan site of Barranco León (Orce, Andalusia, Spain): The fundamental role of pounding activities in hominin lifeways. *Journal of Archaeological Science, 96*, 131–147. https://doi.org/10.1016/j.jas.2018.06.004

Titton, S., Oms, O., Barsky, D., Bargalló, A., Serrano-Ramos, A., García-Solano, J., Sánchez-Bandera, C., Yravedra, J., Blain, H.-A., Toro-Moyano, I., Jiménez Arenas, J. M., & Sala-Ramos, R. (2021). Oldowan stone knapping and percussive activities on a raw material reservoir deposit 1.4 million years ago at Barranco León (Orce, Spain). *Archaeological and Anthropological Sciences, 13*, 108. https://doi.org/10.1007/s12520-021-01353-w

Toro-Moyano, I., Barsky, D., Cauche, D., Celiberti, V., Grégoire, S., Lebegue, F., Moncel, M. H., & Lumley, H. (2011). The archaic Stone tool industry from Barranco León and Fuente Nueva 3 (Orce, Spain): Evidence of the earliest hominin presence in southern Europe. *Quaternary International, 243*, 80–91. https://doi.org/10.1016/j.quaint.2010.12.011

Toro-Moyano, I., Martínez-Navarro, B., Agustí, J., Souday, C., Bermúdez de Castro, J. M., Martinón-Torres, M., Fajardo, B., Duval, M., Falguères, C., Oms, O., Parés, J. M., Anadón, P., Julià, R., García-Aguilar, J. M., Moigne, A. M., Espigares, M. P., Ros-Montoya, S., & Palmqvist, P. (2013). The oldest human fossil in Europe, from Orce (Spain). *Journal of Human Evolution, 65*(1), 1–9. https://doi.org/10.1016/j.jhevol.2013.01.012

Treves, A., & Palmqvist, P. (2007). Reconstructing hominin interactions with mammalian carnivores (6.0–1.8 Ma). In S. L. Gursky,

& N. Kai (Eds.), Primate anti-predator strategies (1st ed., pp 355–381). *Developments in Primatology Series: Progress and Prospects.* Springer, New York.

Treves, A., & Naughton-Treeves, L. (1999). Risk and opportunity for humans coexisting with large carnivores. *Journal of Human Evolution, 36*(3), 275–282. https://doi.org/10.1006/jhev.1998.0268

Turq, A., Martínez-Navarro, B., Palmqvist, P., Arribas, A., Agustí, J., & Rodríguez-Vidal, J., (1996). Le Plio-Pleistocene de la region d'Orce, Province de Grenade, Espagne: bilan et perspectives de recherche. *Paleo* 8, 161–204. https://www.persee.fr/doc/pal_1145-3370_1996_num_8_1_911

Valli, A. M. F., Caron, J.-B., Debard, E., Guérin, C., Pastre, J.-F., & Argant, J. (2006). Le gisement paléontologique villafranchien terminal de Peyrolles (Issoire, Puy-de-Dôme, France): Résultats de nouvelles prospections. *Geodiversitas, 28*(2), 297–317. https://doi.org/10.5281/zenodo.5373488

Wagner, S., Eckmeier, E., Skowronek, A., & Günster, N. (2015). Pedogenetic processes and pedostratigraphy of the Quaternary on the Balearic Islands and in the Granada Basin, Spain. *Quaternary International, 376*, 134–145. https://doi.org/10.1016/j.quaint.2015.01.036

Wu, W., & Wang, S. S. Y. (2006). Formulas for sediment porosity and settling velocity. *Journal of Hydraulic Engineering, 132*(8), 858–862. https://doi.org/10.1061/(ASCE)0733-9429(2006)132:8(858)

Xu, Y.-S., Shen, S.-L., & Du, Y.-J. (2009). Geological and hydrogeological environment in Shanghai with geohazards to construction and maintenance of infrastructures. *Engineering Geology, 109*(3–4), 241–254. https://doi.org/10.1016/j.enggeo.2009.08.009

Yaalon, D. H. (1997). Soils in the Mediterranean region: What makes them different? *CATENA, 28*, 157–169. https://doi.org/10.1016/S0341-8162(96)00035-5

Yravedra, J., Courtenay, L. A., Gutiérrez-Rodríguez, M., Reinoso-Gordo, J. F., Saarinen, J., Égüez, N., Luzón, C., Rodríguez-Alba, J. J., Solano, J. A., Titton, S., Montilla-Jiménez, E., Cámara-Donoso, J., Herranz-Rodrigo, D., Estaca, V., Serrano-Ramos, A., Amorós, G., Azanza, B., Bocherens, H., DeMiguel, D., Fagoaga, A., García-Alix, A., González-Quiñones, J. J., Jiménez-Espejo, F., Kaakinen, A., Munuera, M., Ochando, J., Piñero, P., Sánchez-Bandera, C., Viranta, S., Fortelius, M., Agustí, J., Blain, H.-A., Carrión, J., Barsky, D., Oms, O., Mallol, C., & Jiménez-Arenas, J. M. (2024). Not seen before. Unveiling depositional context and *Mammuthus meridionalis* exploitation at Fuente Nueva 3 (Orce, southern Iberia) through taphonomy and microstratigraphy. *Quaternary Science Reviews,* 329, 108561. https://doi.org/10.1016/j.quascirev.2024.108561

Yravedra, J., Solano, J. A., Courtenay, L. A., Saarinen, J., Linares-Matás, G., Luzón, C., Serrano-Ramos, A., Herranz-Rodrigo, D., Cámara, J. M., Ruiz, A., Titton, S., Rodríguez-Alba, J. J., Mielgo, C., Blain, H.-A., Agustí, J., Sánchez-Bandera, C., Montilla, E., Toro-Moyano, I., Fortelius, M., … Jiménez-Arenas, J. M. (2021). Use of meat resources in the Early Pleistocene assemblages from Fuente Nueva 3 (Orce, Granada, Spain). *Archaeological and Anthropological Sciences, 13*, 213. https://doi.org/10.1007/s12520-021-01461-7

Yravedra, J., Solano, J. A., Herranz-Rodrigo, D., Linares-Matás, G. J., Saarinen, J., Rodríguez-Alba, J. J., Titton, S., Serrano-Ramos, A., Courtenay, L. A., Mielgo, C., Luzón, C., Cámara, J., Sáncjez-Bandera, C., Montilla, E., Toro-Moyano, I., Barsky, D., Fortelius, M., Agustí, J., Blain, H.-A., … Jimenez-Arenas, J. M. (2022). Unravelling hominin activities in the zooarchaeological assemblage of Barranco León (Orce, Granada, Spain). *Journal of Paleolithic Archaeology, 5*, 6. https://doi.org/10.1007/s41982-022-00111-1

Authors and Affiliations

Paul Palmqvist[1] · Isidoro Campaña[1] · Alejandro Granados[1] · Bienvenido Martínez-Navarro[2,3,4] · Alejandro Pérez-Ramos[1] · Guillermo Rodríguez-Gómez[5,6] · Antonio Guerra-Merchán[1] · Sergio Ros-Montoya[1] · María Dolores Rodríguez-Ruiz[7] · José Manuel García-Aguilar[1] · Víctor Hernández[8] · M. Patrocinio Espigares[1]

✉ Paul Palmqvist
ppb@uma.es

✉ M. Patrocinio Espigares
mpespigares@uma.es

[1] Departamento de Ecología y Geología, Facultad de Ciencias, Universidad de Málaga. Campus Universitario de Teatinos, 29071 Málaga, Spain

[2] IPHES-CERCA, Institut Català de Paleoecologia Humana I Evolució Social. C/ Marcel.Lí Domingo, S/N. Campus Sescelades, Edifici, W3. 43007 Tarragona, Spain

[3] Area de Prehistoria, Universitat Rovira I Virgili. Avda. Catalunya, 35. 43002 Tarragona, Spain

[4] ICREA. Pg. Lluís Companys, 23. 08010 Barcelona, Spain

[5] Departamento de Geodinámica, Estratigrafía y Paleontología, Universidad Complutense de Madrid. C/ José Antonio Novais, 12. 28040 Madrid, Spain

[6] Centro UCM-ISCIII de Evolución, Comportamiento Humanos. Avda. Monforte de Lemos, 5, Pabellón 14, 28029 Madrid, Spain

[7] Departamento de Química Inorgánica, Cristalografía y Mineralogía, Facultad de Ciencias, Universidad de Málaga. Campus Universitario de Teatinos, 29071 Málaga, Spain

[8] Departamento de Química Física, Facultad de Ciencias, Universidad de Málaga. Campus Universitario de Teatinos, 29071 Málaga, Spain